Technical Report HCSU-106

# CAMERA TRAP DISTANCE SAMPLING SURVEY DESIGN, ANDERSEN AIR FORCE BASE, GUAM

Richard J. Camp[1] and Trevor M. Bak[2]

[1] U.S. Geological Survey, Pacific Island Ecosystems Research Center, Kīlauea Field Station, P.O. Box 44, Hawai‘i National Park, HI 96718
[2] Hawai‘i Cooperative Studies Unit, University of Hawai‘i at Hilo, P.O. Box 44, Hawai‘i National Park, HI 96718

Hawai‘i Cooperative Studies Unit
University of Hawai‘i at Hilo
200 W. Kawili St.
Hilo, HI 96720
(808) 933-0706

July 2023

Citation: Camp, R. J., and T. M. Bak. 2023. Camera trap distance sampling survey design, Andersen Air Force Base, Guam. Hawai‘i Cooperative Studies Unit Technical Report HCSU-106. University of Hawai‘i at Hilo. 62 pages. https://hdl.handle.net/10790/5389

This product was prepared under Cooperative Agreement CAG18AC00095 for the U.S. Geological Survey Pacific Island Ecosystems Research Center.

*This article has been peer reviewed and approved for publication consistent with U.S. Geological Survey Fundamental Science Practices (http://pubs.usgs.gov/circ/1367/). Any use of trade, firm, or product names is for descriptive purposes only and does not imply endorsement by the U.S. Government.*

## TABLE OF CONTENTS



## LIST OF TABLES

## LIST OF FIGURES

## ABSTRACT

Reliable population estimates of animal density is one of the most elementary needs for the control and management of wildlife, particularly for introduced ungulates on oceanic islands. On Guam, Philippine deer (*Rusa marianna*) and wild pigs (*Sus scrofa*; wild boar and descendants of domestic pigs) cause agricultural and ecological damage and are hunted for recreational, nutritional, and cultural uses. Most common population estimation methods are based on capture-recapture and related methods that require marking or uniquely identifying individuals. Capturing, marking, and either recapturing or resighting individuals repeatedly is labor intensive and expensive. In many situations marking or individually distinguishing animals is not feasible, necessitating estimating densities and abundance from unmarked animal populations. Motion-triggered camera traps are a relatively low-cost approach that can be used to generate presence/pseudo-absence and indices of relative abundance on multiple species simultaneously. We used distance sampling with camera traps to estimate deer and pig densities from non-independent observations of unmarked animals while accounting for imperfect detection where some present individuals are not detected. We present methods to (1) process the digital imagery data automatically for species detection and species categorization using a machine learning algorithm, (2) automatically estimate distance to detected species using a separate machine learning algorithm, and (3) estimate densities using distance sampling with camera trap methods. We compare accuracy statistics and results of ungulate densities estimated from automated methods to those estimated from manual assessment. We collected 7,695 videos: 381 videos contained deer and 377 contained pigs. The object detection and identification model performed well with overall accuracy above 80% and F1 scores above 0.9. The hazard-rate key detection function was chosen for deer and pigs based on Akaike's information criterion accounting for overdispersion. Deer density estimates were 0.53 ± 0.20 deer/ha with higher density in the Plateau area than the Tarague area of Guam. Pig density estimates were 0.53 ± 0.32 pigs/ha, also with higher densities in the Plateau area than the Tarague area. Coefficients of variation ranged from 0.38 to 1.15, and greater numbers of camera traps would be required for pigs than deer to achieve desired coefficients of variation. On average, 101.9 ± 82.3 deer and 131.6 ± 118.8 pigs were detected per day. Microsite heterogeneity affected densities where orientation-specific estimates were less precise than estimates made with the full dataset. We developed a camera trap survey design based on standard camera trapping sampling protocols using motion-activated, digital cameras and determined that distance sampling methods using camera traps produce reliable densities of unmarked deer and pigs on Guam. Our camera trap survey design is based on a regularly sized trapping grid that is generalizable and can be expanded to survey other areas of Guam.

## INTRODUCTION

Obtaining accurate population estimates is one of the most elementary needs for the control and management of wildlife, particularly introduced ungulates on oceanic islands. On Guam (known as Guåhan in the Chamorro language), Philippine deer (*Rusa marianna*; Wiles 2012) and wild pigs (*Sus scrofa*; wild boar and descendants of domestic pigs; Hess *et al.* 2020) cause agricultural and ecological damage and are hunted for recreational, nutritional, and cultural uses. In areas of high conservation value, land managers are required to control and eradicate ungulates including forests on the Naval Magazine, Naval Communications Station, Naval Facility, and Andersen Air Force Base military bases (JRMNRS 2012). In other areas of the island, the Guam Division of Aquatic and Wildlife Resources is tasked with the management of both ungulates as game species. Understanding population size, and the relative proportion harvested, is important for maintaining sustained hunting.

Methods to estimate ungulate densities are intensive. The most common methods are based on capture-recapture and related methods that require uniquely identifying individuals (Amstrup *et al.* 2005, Royle *et al.* 2014) to generate individual encounter history data. Capturing, marking, and either recapturing or resighting individuals repeatedly requires substantial time, field crew, and financial costs. As such, most available capture-recapture methods are difficult to implement, particularly in mountainous and tropical environments. Logistics, safety, and financial constraints often limit which methods and sampling intensity can be used, and the duration sustained.

Naval Facilities Engineering System Command Marianas (NAVFACMAR), Andersen Air Force Base (AAFB), Guam, requested a survey design to estimate ungulate (Philippine deer and wild pig) densities in areas where ungulates will be eradicated or controlled and, after control, monitored to determine management efficacy. Here we develop a survey design that is flexible and includes guidance to collect and analyze camera trapping data to estimate ungulate abundances.

Capture-recapture methods using remotely triggered cameras (camera traps) is a relatively low-cost approach that can be used to generate presence/pseudo-absence and indices of relative abundance on multiple species simultaneously (Royle *et al.* 2014). Camera traps are minimally invasive and can obtain information on rare or cryptic species inhabiting a wide range of habitats (Steenweg *et al.* 2017). As a result, the use of camera traps has increased substantially over the last decade (Rovero and Zimmermann 2016), and the method has become a standard tool for wildlife population monitoring such as wild boar across Europe (ENETWILD-consortium *et al.* 2019).

Relative abundance using site occupancy or detection rate are easily generated from camera trap data and are commonly used as an index of abundance, a measure of relative abundance (Parsons *et al.* 2017). Relative abundance is assumed to have a direct, linear, and constant relationship with wildlife density (Pollock *et al.* 2002); however, this assumption is rarely realistic due to heterogeneity in detection rates across space and time because of changes in environmental conditions, animal behavior, or study methods (Sollmann *et al.* 2013, Parsons *et al.* 2017). Despite good correlation between detection rates and density for many ungulate species, a large body of literature shows that factors other than density affect the number of animals photographed or captured on camera traps, and the consensus is that methods to estimate abundance accounting for imperfect detection is preferred to methods that rely on indices (Kays *et al.* 2020).

The Philippine deer was purposefully released on Guam for the purposes of providing food and recreational hunting (Wiles *et al.* 1999). The Philippine deer is a medium-sized deer native to the Philippines and was introduced to Guam probably in 1771. Deer are prolific, breed year-round on Guam, produce one fawn per birth, and, although the population varies across the island, Wiles *et al.* (1999) noted that densities of > 60 deer/km$^2$ have been recorded. Deer cause agricultural and ecological damage resulting in trampling, over browsing, substantial damage to native plants, and changes in forest composition and structure. Moreover, hunters and poachers regularly burn grasslands to attract deer to new plant growth (Wiles *et al.* 1999), which causes further ecological damage including conversion of forest to grassland and soil erosion that harms freshwater streams and coral reefs (Tribble *et al.* 2016). Deer are hunted on Guam with legal harvests of 600–1,000 deer per year (JRMNRS 2012), and illegal harvest likely exceeds legal harvest (Wiles *et al.* 1999). Control of deer is possible through intensive, continuous harvest over large areas, whereas a program of fencing, hunting, and snaring is effective for eradication of deer in smaller areas.

The wild pig is native to Europe, Asia, and North Africa, and was introduced to Guam in the late 1600s as a food source (Conry 1988). Pigs are prolific, breed year-round on Guam, produce four to six piglets per litter, have about 1.5 litters per year, and may reach densities of 110 pigs/km$^2$ (Conry 1988; although Conry was circumspect of this estimate). In addition to agricultural and ecological damage through browsing and trampling, pigs wallow, dig, and root in soil causing substantial damage to native plants and changes in forest composition and structure. Controlling pigs is more challenging than controlling deer due to prolific reproductive rates of pigs and difficulties of removing the last individuals. Similar management practices to control deer are effective for pigs, although intensity can be substantially different.

## CAMERA TRAP DISTANCE SAMPLING

In many situations it is not feasible to mark or individually distinguish animals, requiring estimating densities and abundance of unmarked animal populations. Estimating animal abundance with data from camera traps has emerged as a valuable approach in the absence of identifiable individuals (Palencia *et al.* 2021). The distance sampling with camera traps (CTDS) method allows for non-independent observations of multiple detections of an unmarked animal and imperfect detection where some present individuals are not detected (Howe *et al.* 2017).

Distance sampling has a well-described theoretical framework and is a core wildlife monitoring method for estimating densities of unmarked populations (Buckland *et al.* 2001, 2004, 2015; Thomas *et al.* 2010). In general, distance sampling involves surveying transects or points, measuring the horizontal or radial distance to detected animals, and fitting a detection function to the distances to estimate densities using a Horvitz-Thompson-like estimator. At predetermined points, the horizontal distance to detected animals is measured, and a detection function is fitted to a histogram of the distance measurements assuming that detection decreases with increasing distance and accounting for imperfect detection. Howe *et al.* (2017) extended the point-transect distance sampling model to accommodate camera trap data and formulated the CTDS method. The adaptation is that camera traps instead of humans are the observers. For CTDS, stationary cameras detect animals as they move through the camera's field of view (Howe *et al.* 2017). Thus, additional information beyond the number of animals detected is needed: a measurement of each camera's field of view; a calibrated measurement of the distance to each detected animal; and the temporal sampling effort summed across all cameras (Hofmeester *et al.* 2017, Howe *et al.* 2017).

Density and abundance estimates using distance sampling methods are unbiased when critical assumptions are met (Buckland *et al.* 2015). For CTDS, assumptions are that the detectors are randomly located relative to animals, animals at distance 0 are perfectly detected, the probability of detecting an animal decreases with increasing distance from the camera, animals are detected at their initial location, distances are measured accurately, and detections are independent events (Buckland *et al.* 2001, 2015). The first five assumptions can be achieved with a robust study design and sampling procedures. The independence assumption is violated when measuring distances to each detected animal multiple times and introduces overdispersion; however, the independence assumption can be met during the model selection stage using a two-step model selection process and estimates generated from bootstrap procedures (Howe *et al.* 2019; details are described below). Specific to CTDS, estimates are unbiased only when the study species is active and available for detection (Howe *et al.* 2017). The common approach to achieve this assumption is to determine the species' activity pattern and censor times when animals are not active or available (Howe *et al.* 2017, Cappelle *et al.*

2019, Gilbert *et al.* 2021). CTDS has been used to estimate populations of Maxwell's duiker (*Philantomba maxwellii*; Howe *et al.* 2017), western chimpanzee (*Pan troglodytes verus*; Cappelle *et al.* 2019), bighorn sheep (*Ovis canadensis*; Harris *et al.* 2020), Alpine marmot (*Marmota marmota*; Corlatti *et al.* 2020), a community of rainforest species (Bessone *et al.* 2020, Cappelle *et al.* 2021), and group-living and solitary mountain ungulates (Pal *et al.* 2021).

ENETWILD-consortium *et al.* (2019), Gilbert *et al.* (2021), and Palencia *et al.* (2021) provide detailed reviews of camera trap methods to estimate densities of unmarked animals. Here we summarize why alternative models were considered and disregarded for this survey design. ENETWILD-consortium *et al.* (2019) evaluated 18 direct and indirect methods to estimate boar density and concluded that indirect methods were too costly and required collecting additional ancillary data to produce accurate estimates. Direct methods of camera trapping using random encounter model drive counts and distance sampling with thermography were recommended for estimating local-scale densities. The random encounter model requires an accurate estimate of the species daily range within the study area (Rowcliffe *et al.* 2008, Lucas *et al.* 2015), and extrapolating densities for the sampling frame is problematic. Animal movement patterns and speed information are not readily available for either deer or wild pigs on AAFB where telemetry data of global positioning system (GPS) locations and movement data were collected every four hours (S. Vogt and A. Rieffanaugh, NAVFACMAR, written communication, 2 March 2021). Drive counts require high effort with estimates dependent on weather, animal density, experience, and availability, and personnel experience, coordination, and motivation. Distance sampling with thermography uses line transect distance sampling methods that may be unreliable with low densities, dense understory, and when the transect center line cannot be clearly marked, which are common conditions in distance sampling-based datasets, particularly those in tropical environments (Buckland 2006, Camp *et al.* 2009).

Gilbert *et al.* (2021) and Palencia *et al.* (2021) reviewed five additional methods to estimate density from camera trap data. Site-structured models, including N-mixture (Kéry and Royle 2016) and Royle-Nichols (Royle and Nichols 2003) models, do not readily allow for predicting abundance and are sensitive to assumption violations, and Link *et al.* (2018) suggest that site-structured models should be treated as indices of relative abundance. Time-to-event models (Moeller *et al.* 2018) rely on restrictive assumptions of perfect detection, which is rarely valid, and that animals are distributed according to a Poisson process, and a biologically meaningful sampling frame needs to be defined instead of sampling frames based on management units (Gilbert *et al.* 2021). Space-to-event and instantaneous sampling (Moeller *et al.* 2018) methods are extensions of time-to-event models and share the same limitations. Moreover, when ungulate numbers occur at low densities, few or no detections may be recorded making inference from the methods unattainable.

Nakashima *et al.* (2018) modified random encounter models by substituting the speed of movement for the amount of time an animal remains within a specific area within the camera trap field of view, termed staying time, to produce a random encounter staying time model. The random encounter staying time model has the same assumptions, sampling design considerations, and extrapolation issues as random encounter models. Spatial counts (also called unmarked spatial capture-recapture; Chandler and Royle 2013, Evans and Rittenhouse 2018) estimate density by modeling the number and distribution of animal activity centers, which requires spatially correlated detection data and arrays of cameras. Unmarked spatial capture-recapture methods are computationally expensive and sensitive to assumption violations and choice of priors and produce highly imprecise density estimates (Gilbert *et al.* 2021).

The CTDS method is useful for monitoring solitary or groups of elusive species, nocturnal species, and species that cannot be readily marked or where individuals cannot be uniquely identified, and it produces superior quantitative and qualitative results to other methods.

Palencia *et al.* (2021) compared random encounter, random encounter staying time, and CTDS methods and recommends the random encounter staying time method for high abundance populations, the CTDS method for low abundance populations, and the random encounter method when camera trap performance is suboptimal. Palencia *et al.* (2021) did not find significant differences in independent and CTDS estimated densities in five out of six multispecies populations and conclude that CTDS may have underestimated densities of wild pigs in the sixth population. Although the simulation and duiker studies of Howe *et al.* (2017) and multi-species study of Palencia *et al.* (2021) are not definitive, they indicate a consistency of CTDS methods to estimate unbiased densities of unmarked populations. Based on the decision tree by Gilbert *et al.* (2021), distance sampling with camera traps is the most appropriate method for estimating densities of unmarked deer and pig populations on AAFB. More generally, CTDS is appropriate for estimating densities of unmarked ungulates elsewhere on Guam and is the preferred method used in this survey design. CTDS is a multi-phase model of (1) data collection, (2) data processing and classification, and (3) density estimation. Here, we provide a detailed survey design to conduct CTDS sampling, methods to process the digital imagery data collected to estimate distances to ungulates, and methods to estimate deer and pig densities with variance using CTDS.

## SURVEY DESIGN

A sampling design is needed to estimate deer and wild pig densities before and after management actions are implemented to determine management efficacy in areas where they will be controlled. The design is based on using trail cameras (hereafter camera traps), which cannot differentiate among individuals but permit identification by species. The sampling design is planned to be deployed on AAFB, and CTDS estimates can be compared with known ungulate densities to assess estimator bias and uncertainty. The sampling design can be expanded as needed to estimate ungulate densities in unfenced areas, permitting ingress and egress movement.

The primary objective of this study was to produce unbiased and precise density estimates of wild deer and pigs in areas with closed and open populations. Change in densities resulting from ungulate control programs requires precise estimates that allow for detecting reductions in abundance over short intervals, time periods relevant for management purposes. Based on discussions with Scott Vogt and Aaron Rieffanaugh, the sampling design is expected to permit detecting a 25% reduction in densities in five years. This typically requires uncertainty in the estimator to be small with a coefficient of variation (CV) in the 0.1 to 0.2 range.

Guam is in the west-central Pacific (13º 28′ N, 145º 00′ E) and is the southernmost island of the Mariana archipelago. The island is about 45 km long, ranges between 6 and 13 km wide, and encompasses about 541 $km^2$. Major vegetation includes native limestone forest, secondary forest, and savanna (Amidon *et al*. 2017). Temperatures are warm, ranging annually from 22º C to 33º C, and wet with average annual rainfall exceeding 2,000 mm, which predominantly falls during the wet season from July to November (Lander and Guard 2003). The study was conducted on AAFB at the north end of Guam.

### Data Collection

To be comparable across space and time, following standardized approaches for CTDS studies is important. This allows for the study and monitoring of wildlife populations across a wide range of habitats, latitudes, and management activities.

**Cameras and Digital Data**
The design uses standard trail cameras. Camera trapping consists of an array of fixed cameras that are triggered by infrared sensors to take photographs or videos of animals passing in front of them. Available data types include still shots and video. The type of data will influence the amount of data collected, storage requirements, and processing and handling (Young *et al.* 2018). Regardless of the data type, classification of a large accumulation of images is required. Traditionally classification of imagery was completed manually; however, recent advances such as machine-learning methods have substantially reduced classification time and made classification methods repeatable (Tabak *et al.* 2019).

**Sampling Frame**
A sampling frame is the list of sample units from which a sample is drawn. Because of the dynamic nature of controlling and eradicating ungulates, the sampling frame will vary among studies and management activities. Unless CTDS is applied to a discrete area (e.g., a fenced management unit), the sampling frame will not be well-defined resulting in a subjective definition of sampling units and limiting generalizations of results to a target population. An undefined sampling frame could lead to different outcomes. This highlights the need for careful consideration in the definition of the sampling frame and sampling units. Beyond management activities and units, land use, forest type, and cover can be used to define the sampling frame (Hofmeester *et al.* 2019). When many sites are surveyed, post-stratification methods can then be used to estimate strata-specific densities (Buckland *et al.* 2015).

**Availability**
Camera traps detect only moving animals within the range of the camera sensor and field of view. Thus, CTDS requires an estimate of the proportion of time animals are available for detection (termed availability; Howe *et al.* 2017). Availability can be affected by the sampling and peak activity periods. CTDS methods can be sensitive to temporal variation in animal activity patterns. When the animals' activity patterns are accounted for, the CTDS estimator is unbiased (Howe *et al.* 2017). Censoring the effort and distance data can improve the estimator, and knowledge of the target animal movement characteristics and density-dependent movement behavior can help minimize bias and violations of model assumptions. An alternative approach to censoring the data is to multiply densities by the proportion of time when animals are available (Howe *et al.* 2017, Nakashima *et al.* 2018).

**Sampling Period**
CTDS does not require the assumption of closure where the population size does not change due to births and deaths or immigration and emigration that standard capture-recapture methods require. If abundance does change during the survey, CTDS will provide an average density across the sampling period (Palencia *et al.* 2021). Restricting sampling to a narrow period facilitates detecting changes in populations and evaluating the effectiveness of management activities.

Seasonal detectability is prevalent, even in tropical environments where species lack migration, hibernation, or seasonally caching food behaviors (Rowcliffe *et al.* 2011). Temperatures in tropical climates vary relatively little seasonally. Seasonal rainfall patterns can be pronounced with alternating wetter and drier seasons (Primack and Corlett 2005, Ghazoul and Sheil 2010). The concern is that animal activity patterns and movements will vary between wet and dry seasons; however, several camera trap studies found little evidence that animal occupancy and detectability varied significantly between seasons (Martin *et al.* 2017), whereas other studies found that activity decreased in the wet season (Rovero *et al.* 2014).

**Peak Activity Period**

CTDS methods can be sensitive to temporal variation in animal activity patterns and require limiting the sampling period to the portion of the day when animals are available for detection (peak activity; Howe *et al.* 2017). Rowcliffe *et al.* (2014) provides a quantitative approach to estimating animal activity using time-of-detection data from camera traps. The key assumptions are that all individuals are active, and therefore available to be sampled, at the peak of the daily activity cycle, a synchrony assumption, and that camera trap locations are random with respect to diel patterns of movement and the daily activity cycle. The R package *activity* (Rowcliffe 2021) facilitated determining peak activity level. We analyzed previously collected still shot images to determine if deer and pig availability differs among study areas and times (Appendix I). For most studies, pooling detections across all sites and times is needed to achieve sufficient sample sizes to reliably model peak activity levels. In practice, this may obscure discerning activity levels in particular areas and minimize heterogeneity in activity levels among trap sites. Incorporating the proportion of animals active throughout the sampling period in the density estimator can minimize small sample size concerns and capture variability among sites.

**Camera Deployment**

*Adequate coverage (number of cameras)*

How many cameras to deploy is a tradeoff among providing adequate coverage to capture spatial heterogeneity (Kays *et al.* 2021), obtaining sufficient numbers of detections to reliably fit a detection function (Buckland *et al.* 2015, Howe *et al.* 2017), and avoiding collecting and processing more images than is necessary to produce precise population estimates (Corlatti *et al.* 2020). Study designs that use a consistent arrangement generally reduce variation among camera trap sampling units and may detect species with clustered distributions or with nonuniform spatial activity patterns (Evans *et al.* 2019). A systematic random design is recommended for point-transect distance sampling (Buckland *et al.* 2015). As a variation on point-transect distance sampling methods, CTDS inherits its features. Therefore, a regular grid with random origin is the recommended design for CTDS. Each intersection on the grid is a camera trap site where the number of camera trap sites sampled is defined by the distance among grid intersections within the study area.

*Trapping effort*

Trapping effort is defined as the number of trap nights or camera days in a camera trap survey (Kelly 2008) and is an important metric for designing efficient studies. Trapping effort is directly related to distance sampling via how many detections are recorded given a set number of camera trap sites operated for a given period of time. Buckland *et al.* (2015) recommends collecting at least 75 to 100 detections to reliably model detection functions. Trapping effort is affected by habitat, weather conditions, abundance of target species, and spacing of cameras (Si *et al.* 2014).

*Placement of trap locations*

Methods of CTDS assume that the trap locations are randomly located, usually following a random or systematic random design (Buckland *et al.* 2015), and that the orientation of cameras is also random (Howe *et al.* 2017). Randomized placement is a design-based requirement of distance sampling to provide inference from the sample to the population. A systematic random design of trapping points laid out on a grid with a random origin is preferred to a completely random design. In addition to being more straightforward than complete random sampling, a systematic random design is more conducive to sampling over a wide area, can provide maximum spatial coverage, and can facilitate mapping spatial patterns in ungulate distributions and abundances. Moreover, a systematic random design provides a more robust sampling strategy for inferences to larger scales including study, regional and island-wide populations. The disadvantage of using a systematic random design is over- or under-representation of particular habitats.

Random orientation ensures that habitats are sampled representatively, regardless of animal movement and if animals either bypassed or preferentially used the sampled space (i.e., sample well-established trails; Rowcliffe *et al.* 2014, Kays *et al.* 2021). Preferential placement of camera traps and orientation of cameras should be avoided. In practice, however, traps should be placed close to the theoretical position and systematically oriented towards the most naturally cleared area (Fonteyn *et al.* 2020). Palencia *et al.* (2021) included camera locations that were up to 80 m from the theoretical position on a grid with 1.5- or 2-km spacing. This was done to mount cameras on trees and avoid unfavorable conditions of dense understory. Most trapping grids on AAFB and Guam will have shorter spacing distances; thus, the realized trap location should be within a distance of about 5% from the theoretical location (80 m/1.5 km). All camera traps were established within a few meters of the grid intersections.

A standard practice to minimize recordings triggered by movement of vegetation is to orient cameras toward naturally cleared areas, which ensures that animals throughout the field of view (FOV) can be sampled and the transmission of infrared radiation towards the sensor is uninhibited (Hofmeester *et al.* 2017). This procedure also reduces heterogeneity in detection probability across individuals. Fonteyn *et al.* (2020) recommends cutting back vegetation within a 3-m radius of the camera to reduce false triggers and ensure detection is certain at zero distance. The undergrowth should, however, remain mostly unchanged.

*Length of trap occasions*

Unlike capture-recapture models, the closed population assumption is not relevant for CTDS. A ‘trapping occasion’ is essential for capture-recapture models to generate capture histories that are used to estimate capture and recapture probabilities. Methods for CTDS rely on estimating the detection probability based on the decay of detections with distance, not on generating capture histories where the length of trapping occasions is controlled by the closure assumption. The length of trapping occasions should therefore be long enough to ensure that enough detections are recorded to reliably estimate the detection probability, and based on point-transect distance sampling methods, Buckland *et al.* (2015) recommends at least 75 to 100 species-specific detections. Monitoring can occur across periods when populations are changing such as across the breeding season or periods of high mortality. Animal densities, in these cases, are averages of the changing population yet do not suffer from violation of the closed population assumption (Palencia *et al.* 2021). However, the survey period should be kept relatively short to capture snapshots of the population, and many trapping occasions should be used to describe changes in the population and assess the efficacy of management actions.

*Camera installation and settings*

Cameras should be installed at a low height between the sensor and ground to minimize violations of the certain detection at distance zero assumption (Howe *et al.* 2017, Palencia *et al.* 2021). Haucke *et al.* (2022) recommends that cameras should be tightly secured to stationary objects such as trees to minimize motion, and that the FOV in proximity of the camera should be free of vegetation that could obscure animals or trigger the motion sensor. An additional recommendation Haucke *et al.* (2022) suggests is that the bottom third of the FOV should be of the ground. This view captures individuals within a meter of the camera and provides context information required for the monocular depth estimation.

Based on previous camera trap studies in AAFB, cameras secured to trees 30–50 cm above the ground and angled to be parallel to the slope of the ground recorded animals throughout the FOV, including animals that occurred within a meter or so of the camera (S. Vogt, NAVFACMAR, written communication, 7 December 2021). E. Howe (Ontario Ministry of Natural Resources and Forestry, written communication, 13 January 2022) recommends systematic orientation of cameras starting with north and switching orientation from north to south about halfway through the trapping occasion to increase sampling microsite heterogeneity about the camera trap.

Howe *et al.* (2017) recommends programming cameras to record video or multiple still images each time the sensor is triggered. E. Howe (Ontario Ministry of Natural Resources and Forestry, written communication, 1 April 2021) recommends that the video length should be long enough that some animals can be detected leaving the FOV at the sides. This ensures that the camera angle of view with angle θ radians matches the full camera FOV and not the effective angle of the sensor because the sensors are less effective at the sides of the FOV. Cameras should have fast trigger times (< 0.5 second [s]) and should be set to record a long video at each activation (e.g., 15 s) with a minimum trigger delay between detection events, preferably < 1 s. The cameras should retrigger as long as animals are in the sensor range (Kays *et al.* 2020). In addition, infrared flashes should be used at night to avoid disturbing animals.

*Defining area of camera viewshed*

Density estimation requires defining the proportion of area sampled (Howe *et al.* 2017). The camera angle of view (AOV) can be included as a multiplier in the *dht2()* function of DISTANCE (Miller *et al.* 2019) through the *sample_fraction* argument. The AOV is an absolute measure of the horizontal and vertical angles captured by a camera and is available from the camera manufacturer. The AOV can be affected by visual obstructions and edge-effects—to address this, AOV can be measured in the field as the FOV (how much of the surroundings is captured by a camera). Further, AOV provided by the camera manufacturer can be incorrect when compared to empirical FOV measured in the field, which can bias estimates (Corlatti *et al.* 2020).

*Demarcating distances in the field of view*

Manual methods to estimate distance from detected animals to the camera require demarcating known distances in the FOV. Some automated methods also have this requirement (Haucke and Steinhage 2021, Haucke *et al.* 2022). Standard approaches to manually measure distances to detected animals within the FOV use two methods: (1) visual estimation by reference images or objects; and (2) on-site distance measurement. Visual estimation using reference images commonly entails holding a sign noting the distance and traversing at that distance in the FOV (Howe *et al.* 2017). In addition, distance marks (artificial [Hofmeester *et al.* 2017] or natural [Palencia *et al.* 2021]) can be placed in the FOV that are used to locate the position of captured individuals. Palencia *et al.* (2021) placed natural marks, such as rocks and branches, in the FOV at 2.5-m intervals from the camera trap. Visual estimation by reference images is very laborious and also subjective (Haucke *et al.* 2022). On-site measures require measuring the distances between the camera and the location of each previously captured animal, either with a measuring tape or ultrasonic distance sensor. Although on-site distance measurement is less subjective, returning to each camera trap to obtain measurements to each observed animal is more laborious than visual estimation methods (Haucke *et al.* 2022), and this approach is not recommended.

Placing objects in the FOV at known distances in habitats with an open understory allows for estimating distances that otherwise lack landmarks needed for manual depth estimation methods. Marking objects at known distances in habitats with a closed understory is also advantageous for referencing distances, even if objects are partially obstructed and not completely visible in the FOV. Regardless of understory structure, placing objects and marking landmarks during each camera deployment standardizes manipulating and modifying the surveyed area at all camera traps.

*Sampling*

The CTDS method supports recording either still shot or video images to estimate distances to individuals. Howe *et al.* (2017, 2019) recommends that camera traps should be set to operate continuously, to record a long video at each activation (e.g., 15 s), and to use the minimum triggering interval between activations. The date and time of capture should be automatically stamped onto each video image or would need to be added manually. Camera traps should be checked periodically, every two to three weeks, to change their orientation, batteries, and memory cards.

**Digital Data Processing**

Once camera trap data have been collected, three tasks are performed to (1) determine whether an object is present in the videos; (2) if an object is present, identify the species; and (3) when the species of interest is present, estimate its distance from the camera (Figure 1). Processing the videos can be done either manually or automatically.

*Manual digital data processing*

Manual processing involves visually inspecting each video to determine whether an object is present in the video and if the object is the target species. The distance from the midpoint of each detected animal to the camera is then estimated for all predetermined snapshot moments in which the target species is present. Distances are estimated by comparing animal locations to reference flags and objects in the video (from 1 to 15 m) and to reference images taken at known distances from the camera during camera installation (from 1 to 11 m). Reference images are useful for estimating distances when animals occurred along the sides of the FOV. Distance estimates should be recorded in meter intervals (0 = 0–1 m, 1 = 1–2 m, 2 = 2–3 m, etc.) to minimize measurement errors. Each target species individual entering and exiting the FOV of the camera trap is considered an independent contact. When groups of animals are recorded, each individual is considered a unit of observation. This avoids issues with estimating accurate group size (Palencia *et al.* 2021), and bootstrap methods are used to account for the independence assumption.

*Automated digital data processing*

The use of camera traps in research has grown exponentially in the past decade (Gilbert *et al.* 2021) and with this increase comes enormous volumes of images and videos that need to be processed. Recent advances in machine-learning methods have been utilized to automatically classify camera trap data, increasing the feasibility of processing such large amounts of data (Tabak *et al.* 2019). A wide variety of studies have recently been published utilizing machine learning for object detection (is a species present?) and identification (if yes, what is the species?) of camera trap data with most studies finding high levels of accuracy and large decreases in processing times (Choiński *et al.* 2021, Fennell *et al.* 2022, Tan *et al.* 2022). Ultimately the wide-scale deployment of camera traps along with automated data processing pipelines may enable global real-time monitoring of wildlife populations, a possibility that would be instrumental in helping address biodiversity loss (Steenweg *et al.* 2017).

*Object detection and identification*

The growth of machine learning for object detection and identification has come out of early attempts at image classification such as the landmark study by Krizhevsky *et al.* (2012), which was one of the first to use machine learning to classify a large number of images. Since that study, machine learning object detection and identification has been utilized with increasing

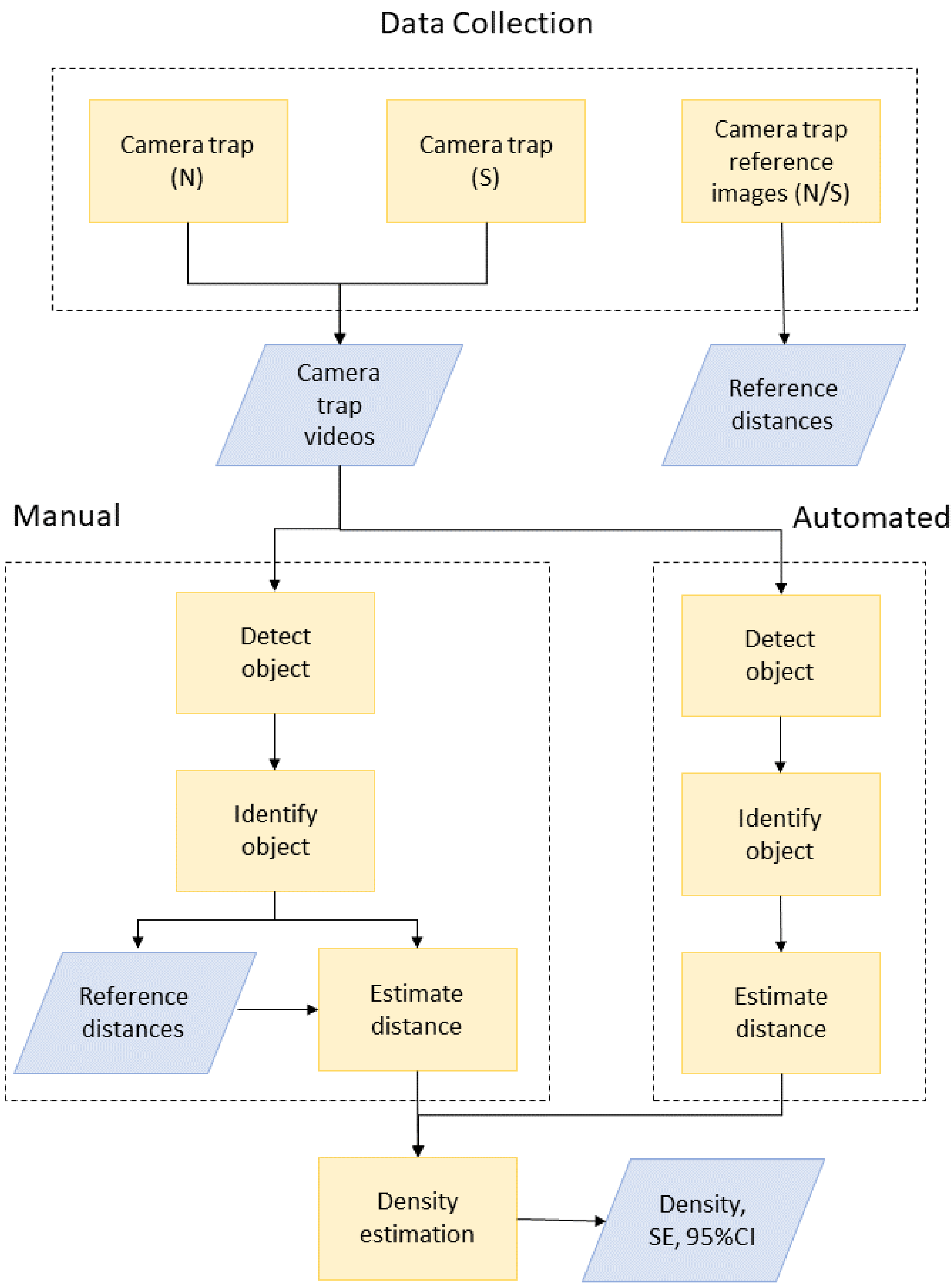


Figure 1. Diagram summarizing the data collection, manual and automated assessment, and density estimation processes. Yellow boxes represent a process, blue trapezoids represent an output, and arrows direct the sequence in processes. Videos from north- (N) and south- (S) oriented cameras are combined to estimate density and measures of uncertainty, standard error (SE), and confidence intervals (95% CI).

accuracy as the models have improved (Fennell *et al.* 2022, Tan *et al.* 2022). Current machine learning algorithms are based on deep neural networks that mimic the way the brain works. Machine learning algorithms can learn quickly and can apply information learned from training data to novel datasets (i.e., novel species and environments; Fennell *et al.* 2022).

For this study we utilized Zamba developed by DrivenData (DrivenData Inc., Denver, Colorado). Zamba is a video object detection and identification program built upon code written for a data science competition. For the competition, data from the "Chimp&See" video set (https://www.zooniverse.org/projects/sassydumbledore/chimp-and-see) was utilized and included over 2,000 hours of video that citizen scientists had manually labeled. Data scientists competed to develop the best machine learning algorithm to detect and identify the wildlife in the videos, and the top three models were used as the starting point for Zamba. In addition to refining the initial machine learning algorithm, the model has also been trained on additional datasets from Africa and Europe.

*Accuracy statistics*

Object detection and identification accuracy statistics are computed to assess model performance. These statistics compare the model-generated labels (e.g., deer, pig, empty) for a given camera image or video to manually assigned labels of the camera trap video object. Common statistics for assessing accuracy are overall accuracy (percent of correct labels), precision (false positives), recall (false negatives), and F1 (balance of false positives and false negatives). Recent testing of models reveals that accuracy is typically over 90% (Fennell *et al.* 2022, Tan *et al.* 2022). Precision is typically in the upper 90% (Fennell *et al.* 2022, Tan *et al.* 2022), and recall is typically in the upper 90% as well (Fennell *et al.* 2022). F1 score is usually in the 80% range (Choiński *et al*. 2021, Fennell *et al*. 2022, Tan *et al*. 2022). Models typically perform better for species they were trained on, and accuracy increases with larger training datasets (Fennell *et al.* 2022). The Zamba model we utilized, the European model, had an accuracy of 80% (https://www.zambacloud.com/).

*Automated distance estimation processing*

Given that distance sampling requires distance estimates of the target animal to the camera, methods to automatically estimate distance with camera trap data have been developed. These methods grow out of earlier pioneering work that explored how to turn two-dimensional (2D) images into three-dimensional (3D) models (Hoiem *et al.* 2005, Saxena *et al.* 2009). This projection of 2D space to 3D space allows for estimation of where objects occur in the image along the third axis, or the depth dimension. Depth estimations have been applied to a range of images (Facil *et al.* 2019) and more recently have been applied to camera trap videos to enable distance sampling analyses (Haucke *et al*. 2022, Johanns *et al.* 2022). A recent advancement in camera trap depth estimation for distance sampling allows for estimating the depth of animals without the need for model calibration based on reference landmarks (Johanns *et al.* 2022). This has the potential to minimize manual processing while allowing for a broader range of camera trap data to be used (Johanns *et al.* 2022).

## Density Estimation

*Model formulation*

Digital data are collected from *k* deployed camera traps (points) that record for as long as an animal is present to trigger the camera. From the digital images, a finite set of 'snapshot moments' within a $T_k$ time period is examined. The snapshots are of predetermined length that are separated by *t* units of time. CTDS methods rely on counts of animals at varying distances from the camera to estimate detection probabilities. In images with the target species, the horizontal radial distance $r_i$ between the camera and the midpoint of the individual is estimated. This continues for the duration the individual remains in view. Each camera covers an angle of view with angle $\theta$ radians. The fraction of the circle covered is $\frac{\theta}{2\pi}$, which is set to effort with a point-specific total sampling effort of $\frac{\theta T_k}{2\pi t}$. Densities are estimated using point-transect distance sampling methods (Buckland *et al.* 2015) with the equation:

$$\widehat{D} = \frac{2t\sum_{k=1}^{K} n_k}{\theta w^2 \sum_{k=1}^{K} T_k \hat{P}_k} \quad \text{Equation 1}$$

where $w$ is the truncation distance and $\hat{P}_k$ is the estimated probability of capturing an animal image within $\theta$ and $w$ of the camera. A detection function is fitted to the histogram of distances $r_i$ to estimate $\hat{P}_k$ following standard distance sampling procedures. Details of the CTDS estimator are provided in Howe *et al.* (2017).

*Model selection*

Distance sampling methods assume that detections are independent; however, distance sampling using cue count and camera-trapping methods may yield over-dispersed data, which are expected to be positively biased due to measuring distances to each detected animal multiple times (Buckland *et al.* 2001, Howe *et al.* 2019). Overdispersion also causes model selection criteria, such as Akaike's information criterion (AIC), to favor overly complex models and can adversely affect estimator accuracy and precision (Howe *et al.* 2019).

Howe *et al.* (2019) proposed a two-step model selection procedure to adjust AIC methods where the adjusted version of AIC (QAIC) is used to select among models with the same general form (i.e., within each key function half-normal or hazard rate models), and then a goodness-of-fit statistic is used to select among models with different forms (i.e., between the best fit key function half-normal or hazard rate models).

Howe *et al.* (2019) provides a detailed description of the two-step model selection procedures. In general, in step one, an overdispersion factor ($\hat{c}$) is computed from the chi-square ($X^2$) goodness-of-fit test of the most highly parameterized model within each key function divided by its degrees of freedom (*df*). The QAIC is then computed using the standard formula where the log likelihood is divided by $\hat{c}$ and the number of parameters is increased by 1 to account for estimating the overdispersion factor. The QAIC is as follows:

$$\text{QAIC} = -2\left\{\frac{\log L(\hat{\theta})}{\hat{c}}\right\} + 2K \quad \text{Equation 2}$$

where log $L$ is the log likelihood value, $\theta$ is a vector of maximum likelihood parameter estimates, and $K$ is the number of parameters in the current model. QAIC is then used to identify the best-fit models within each key function. Howe *et al.* (2019) describes step one as the QAIC1 method. In step two (QAIC2), the model with the smallest $\hat{c}$ value is chosen for estimation.

*Model assumptions*

Camera trap deployment is independent of animal density during the sampling period. This is achieved through randomization following approaches used in point-transect distance sampling. Distance sampling assumptions described by Buckland *et al.* (2015) apply (as described above). Deploying pairs of cameras minimizes issues with detecting animals passing below the FOV of the camera and ensuring detection is certain at zero distance (i.e., all animals at the camera within the AOV are detected with probability 1.0). Left-truncation can also be used in cases where animals in proximity of the camera are missed to minimize bias, although variance can increase substantially.

Animal movement is assumed to be random. This can be met by representatively sampling the landscape and not targeting trails or other features that attract animals (Buckland *et al.* 2015, Howe *et al.* 2017), assuming the snapshot moments are independent of animal locations (as described previously), and specifying predetermined times of day based on periods of peak activity.

*Estimator bias*

In CTDS studies, distances to the first detection of animals are expected to be positively biased (Howe *et al.* 2017). Approaches to account and correct for the bias include programming cameras to either record video or record multiple still images (i.e., bursts of still images) and measure the distances to each detected animal multiple times at predetermined snapshot moments during the encounter. Based on potential bias with multiple still images, Howe *et al.* (2017) recommend setting cameras to record videos. Howe *et al.* (2017) suggest the time between snapshot moments to be between 0.25 and 3 s, with shorter spans for faster-moving animals and cameras that have faster trigger speeds and short recovery times, and longer spans for slower-moving animals and cameras with slower trigger speeds and slower recovery times. Scott Vogt explored using CTDS in a 30-ha fenced area with different lengths of snapshot moments and concluded that snapshot length influenced density estimates, indicating that the estimator may by unreliable when recording multiple still images (S. Vogt, NAVFACMAR, written communication, 10 June 2021).

Bias can occur when animals react to the camera traps and when animals react to cameras being triggered. Attraction or avoidance of camera traps is expected to induce bias (Buckland *et al.* 2015). Howe *et al.* (2017) recommends discarding the first day of the survey to allow animals to become accustomed to the camera traps. In addition, Bessone *et al.* (2020) discarded all the observations where animal behavior indicated a reaction to the camera being triggered. Palencia *et al.* (2021) noted that neither of these approaches solves the reactive animal bias issue and recommended further research. Both deer and pigs on Guam are habituated to humans and accustomed to daily human activities; therefore, discarding detections on the day of deployment and retrieval likely minimizes bias. This approach also allows for evaluating if detections between the first and subsequent days differ (as described in *Trapping Effort*, below).

*Covariates*

Distance sampling methods allow for including covariates, variables that may influence the detectability of animals other than distance (Marques and Buckland 2004). Including covariates in modeling the detection function can improve estimator precision (Marques and Buckland 2004), as well as minimize estimator bias (Hofmeester *et al.* 2019). Plot-level covariates, such as camera type if more than one make or model is used, sampling conditions (e.g., wet or dry season), or stratification by region can be included when modeling the detection function. Sampling covariates are not supported by the *dht2* function at this time; however, stratification can be used to minimize estimator variance and bias.

## METHODS

### Study Area

Camera traps were deployed in two areas of AAFB, an area on the plateau (hereafter Plateau stratum) and on the Tarague bench (hereafter Tarague stratum; Figure 2). The Plateau stratum consisted of hunting and non-hunting units totaling an area of 985 ha. The Tarague stratum included non-hunting areas totaling 410 ha. The Tarague stratum included camera trap points above the cliff line as well as points below the cliff line.

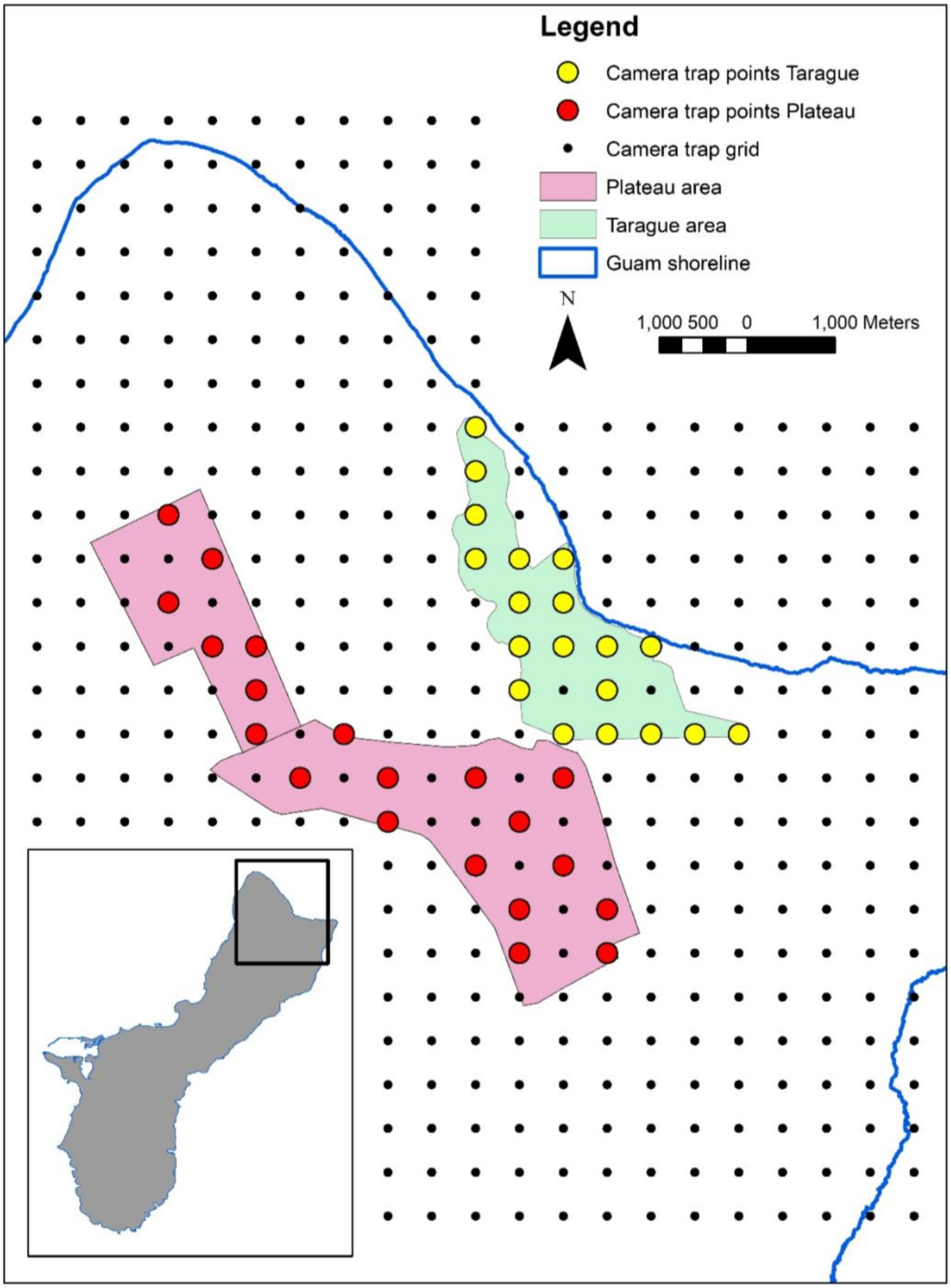


Figure 2. Study area, strata, and layout of camera traps in Andersen Air Force Base, Guam. Black dots are points on a 500- x 500-m regular grid, yellow circles are camera trap points in the Taragué stratum (green polygon), and red circles are camera trap points in the Plateau stratum (pink polygon).

**Camera Installation**

Sampling in our study occurred between 20 January and 9 May 2022, during the dry season (generally December through June). We deployed 24 Moultrie A-Series Digital Game Cameras (Model MCG-13296; PRADCO Outdoor Brands, Calera, Alabama) and 14 Bushnell Trophy Cameras (Model 119876; Bushnell Outdoor Products, Overland Park, Kansas). Camera traps were located at the intersection of a regular 500- x 500-m grid. Camera traps that fell within restricted areas were excluded, and two camera traps that occurred on the edge of restricted areas were relocated < 50 m into the study area. Cameras were secured to trees 30–50 cm above the ground and angled to be parallel to the slope of the ground and to record animals throughout the FOV. We secured each camera to the side of a tree using lag bolts to minimize motion and allow for rotating the orientation of each camera. Digital cameras operated continuously and collected video images when motion was detected by passive infrared sensors. Both cameras used highly sensitive passive infrared motion sensors, set to medium range, and took 1280 x 720 pixels per frame at 20 frames per second images. The Moultrie cameras had a default 15-s video recording length. We programmed the same recording length for all Bushnell cameras except one that recorded 10-s long videos (effort was adjusted appropriately for this camera). Trigger times were programmed to trigger immediately (0.2 s for Bushnell and 0.7 s for Moultrie cameras), and the delay between detections when an animal remained in range was programmed to 0 s. Video images were recorded onto 16GB secure digital high-capacity cards (SD cards; Gigastone, Los Angeles, California). Long-lasting, high performance 1.5 V lithium AA batteries were installed during camera deployment. The SD cards and batteries were checked and replaced when cameras were reoriented.

We used two approaches to determine reference distances. For the first approach we placed survey flags at 1-m intervals from 1 to 15 m and marked natural objects (trees and branches) at known distances from the camera. Our second approach involved a person showing a paper sheet depicting the distance to the camera and walking across the FOV from one side to the other at 1-m intervals between 1 and 11 m.

**Manual Digital Data Processing**

We visually inspected all north-oriented camera video images (n = 1,309) from camera traps with <100 videos to determine if they contained an object and if that object was a target species. The distance from the camera to the center of each individual was estimated when a target species was observed at predetermined snapshot moments. We compared the location of photo-captured individuals to reference distances (first approach, as described above in *Camera Installation*) from the camera. For individuals detected along the sides of the FOV, we compared animal locations to reference images from our second approach (as described above in *Camera Installation*). Distance estimates were recorded in meter intervals (0 = 0–1 m, 1 = 1–2 m, 2 = 2–3 m, etc.). Distances for deer and pigs were compiled separately and used for estimating species-specific detection functions and densities. The predetermined interval between snapshot moments ‘t’ was 2 s (i.e., at 1, 3, 5, …, 15 s), which Howe *et al.* (2017) considered appropriate for fast moving and rare species. For filtering the dataset to peak activity time intervals, we had to record the date and time by hand for all videos with species of interest.

**Automated Digital Data Processing**

For object detection and classification, we used the Zamba Cloud program, version 2.1.0, developed by DrivenData (DrivenData Inc., Denver, Colorado; https://drivendata.co/). For this study we used the European model, due to this model having species (European roe deer [*Capreolus capreolus*] and wild boar) that were similar to our target species of interest, Philippine deer and wild pig. The roe deer is a relatively small deer about 95–135 cm long and 63–67 cm at the shoulder. The wild boar is generally larger than wild pigs on Guam, but otherwise similar in shape. The European model was developed from the African model, which was trained on 250,000 videos from camera traps in Africa. This African model was then trained on an additional ~13,000 videos from camera traps in Germany (https://zamba.drivendata.org/). The European model was trained on a different background (temperate European forest) than our study background (tropical jungle); however, we chose to accept this tradeoff in background generalizability because the European model contains species closer in size and morphology to our target species. We uploaded all non-reference videos to the Zamba website, and DrivenData ran the Python script to identify species in the videos using the European pretrained model. We received a CSV file of predicted species labels for each video. Probabilities were included with each label and indicated how confidently the model predicted the species. Three labels were generated per video, in decreasing order of probability. We used only the first or highest probability label in this analysis.

**Automated Distance Estimation**

For automated estimation of the distance between the camera and observed animal, we used T. Haucke's code described in Johanns *et al.* (2022) and available on GitHub (at https://github.com/PJ-cs/DistanceEstimationTracking). To begin, we split the videos with target species of interest into images at snapshot moments (i.e., at 1, 3, 5, 7, 9, 11, 13, and 15 s in the videos). These snapshot moment images were then processed with MegaDetector (Beery *et al.* 2019) to draw bounding boxes around detected animals. Next, the images were treated with a DINO model (self-distillation with no labels; Caron *et al.* 2021) to create a segmentation mask; that is, an identification of each pixel that makes up part of the animal (i.e., DINO more precisely identifies the animal within the bounding box; Johanns *et al.* 2022). Distances to the segmentation masks are then estimated. A returned CSV file provided an estimated distance for each animal in each image. For images that were not successfully processed, a member of the research team estimated the distances using manual methods described above. Reasons for images not being successfully processed included errors when attempting certain batch file runs, the model generating negative distance estimates, and the model not detecting all instances of multiple individuals (e.g., if there are four pigs in an image and the model only generates distances for two pigs).

**Accuracy Statistics**

To assess Zamba accuracy we manually classified a portion of the videos following methods described above and compared it to the first or highest probability label assigned by Zamba. Then we examined instances in which the Zamba and manual labels disagreed. For images that disagreed we conducted a second manual classification to confirm the correct label and account for rare instances in which Zamba was correct and the manual label was wrong (such as deer at night far away from the camera in which the silhouette was barely visible). We combined the correctly classified labels and classifications that disagreed to assess accuracy.

We used a subset of receiver operating characteristic analyses to assess Zamba model performance (Zou *et al.* 2007), using manual classification after a second round of assessment as the true label. For our purposes we defined a true positive when both automated and manual methods classified a video as having a target species, and a true negative when both methods classified a video as empty or a non-target species. We defined a false positive as a video identified by Zamba as having a target species when the target species was not present, and a false negative as a video identified by Zamba as not having a species of interest when one was present. This permitted computing misclassification errors (e.g., when Zamba identified a video as having a chicken while the animal was identified as a deer during manual classification).

The following accuracy statistics were calculated. Overall accuracy was computed as follows:

$$C = \frac{True\ Positives + True\ Negatives}{Total\ Number\ of\ Videos} \qquad \text{Equation 3}$$

Precision was computed as follows:

$$P = \frac{True\ Positives}{True\ Positives + False\ Positives} \qquad \text{Equation 4}$$

Recall was computed as follows:

$$R = \frac{True\ Positives}{True\ Positives + False\ Negatives} \qquad \text{Equation 5}$$

The F1 score was computed as follows:

$$F1 = 2\left(\frac{P \times R}{P + R}\right) \qquad \text{Equation 6}$$

The precision score represents the rate of false positives to true positives, and the recall score represents the rate of false negatives to true positives. The F1 score is the ratio of false positives and false negatives to true positives and ranges from 0 to 1.

**Period of Activity**

Using every video with a deer or pig, we computed the species-specific peak activity intervals. We accounted for species availability in distance sampling by computing the level of temporal activity with variance (titled All Deer or All Pig) and by sub-setting the dataset to determine species-specific peak activity periods (titled PA Deer or PA Pig). Activity level was estimated using the R package *activity* (Rowcliffe 2021). We fitted the models to clock time because the time of sunrise and sunset varied little over the study period. The time stamp (24:00 clock; hh:mm) for each occurrence was converted to radian time using the *gettime()* function. The level of activity was modeled with the *fitact()* function, and 95% confidence intervals were estimated from bootstrap procedures with 100 iterations. R code for modeling activity levels is available in Appendix II. From visual inspection of the activity level plots we chose the period with maximum continuous activity to subset the dataset to determine species-specific peak activity periods.

**Density Estimation**

We estimated species-specific densities (animals/ha) for deer and pigs using the R (R Core Team 2021) package *distance* (following methods described in Howe *et al.* (2017, 2019). We fit point-transect models of the detection function with the half-normal key function with a Hermite polynomial adjustment term, the hazard rate key function with a cosine adjustment term, and the uniform key function with a cosine adjustment, with expansion series of order two. Sampling covariates are not supported by the *dht2* function. Survey effort at each trap point was the number of $t$ snapshot moments within a $T_k$ time period, restricted to the species-specific peak activity periods. The AOV for Bushnell Trophy Cam[1] was 45º and Moultrie A25[2] AOV was 35º (0.785 and 0.611 radian, respectively). R code for estimating densities using CTDS methods is available in Appendix II. We evaluated model fit through visual inspection of diagnostic plots and excluded fitted detection functions that were not monotonically nonincreasing and when estimated detection probabilities exceeded 1.0 (Buckland *et al.* 2015; Howe *et al.* 2017, 2019).

We selected among candidate models following the two-step procedure described by Howe *et al.* (2019), using the QAIC1 method to identify the best-fit models within each key function. We compared key function models following standard selection methods described by Burnham and

---

[1] https://www.bushnell.com/on/demandware.static/Sites-HuntShootAccessories-Site/Library-Sites-HuntShootAccessoriesSharedLibrary/-/productPdfFiles/bushnellPdf/Product%20Manuals/Trail-Cameras/PDF/119676C_119677C_119678C_TrophyCamHD_1LIM_US-only_052014_web.pdf

[2] https://www.trailcampro.com/pages/trail-camera-detection-field-of-view-angle

Anderson (2002) instead of using the QAIC2 method because $\hat{c}2$ was unknown (refer to Howe *et al.* 2019 for details). Detection function uncertainty was derived from design-based variances ('P3' of Fewster *et al.* 2009, the recommended variance estimator for point-transect distance sampling and associated methods). Total density was computed as the area weighted average of strata-specific densities, and total abundance was computed as the sum of strata-specific abundances. We estimated variances and 95% confidence intervals (CIs) using a nonparametric bootstrap, resampling trap points with replacement from 1,000 iterations.

**Adequate Coverage**

To avoid collecting more images than is necessary for precise population estimates, we evaluated the tradeoff between just enough cameras to capture the spatial heterogeneity in population densities and sufficient numbers of detections to reliably fit a detection function. Achieving adequate statistical power to detect changes in populations requires precise estimates, which can be achieved in part by increasing sampling effort to capture spatial heterogeneity in population densities. We computed the total effort (i.e., number of camera trap points) required to achieve the target coefficient of variation (CV) needed to reliably detect population changes following methods described in Buckland *et al.* (2015, page 24). We computed the total effort for all detections and for peak activity periods. There were $K_0 = 38$ points sampled in which $n_d = 2{,}678$ deer and $n_p = 3{,}637$ pigs were detected. We computed the CV of the species-specific density estimates ($\hat{D}$) as the standard error of the density (SE$(\hat{D})$) divided by CV($\hat{D}_d$) for deer and CV$(\hat{D}_p)$ pigs, and the target CVs (CV$_t(\hat{D})$) of 0.10, 0.20, 0.30, and 0.40. The number of points required to achieve the target CV follows:

$$K = \frac{K_0\{\mathrm{CV}(\hat{D})\}^2}{\{\mathrm{CV}_t(\hat{D})\}^2} \qquad \text{Equation 7}$$

**Trapping Effort**

We examined how the daily detection rate changed with increasing sampling effort to determine how many cameras to deploy and for how long to obtain sufficient detections to reliably fit a detection function (75 to 100 detections recommended by Buckland *et al.* 2015). We also sought to determine an optimal effort of how long cameras are deployed in a given area before the number of detections plateaus. From the regressed weighted cumulative daily detection rates against camera trap days for deer, pigs, and both species combined, we evaluated if breakpoints (the points where the slope in regression segments change) occur in the regression slopes using the *segmented()* function of the package *segmented* (Muggeo 2022).

**Microsite Heterogeneity**

Camera orientation was switched from north to south during the trapping period to increase sampling microsite conditions at camera trap sites. We fitted the best approximating detection function from the full dataset to detections from the north and south orientations separately and compared the CVs.

## RESULTS

We deployed 39 camera traps within the two strata (Figure 2); however, one camera in the Tarague stratum failed to collect any data. Camera traps were deployed on 20 January 2022, and trapping continued until 9 May 2022. Cameras operated between 4 and 34 trap days. Due to logistical constraints, we extended the trapping effort from the proposed two weeks to four months. A total of 14 cameras failed to collect data, either due to battery or SD card malfunctions. These cameras were reset and deployed again. A total of 7,659 videos were recorded and processed.

### Manual Digital Data Processing
We manually assessed 2,376 videos or 31% of all videos for object detection and identification. In our manual assessments we identified 381 deer, 377 pigs, 1,027 empty videos, and 591 other objects (e.g., humans, cats, birds). We manually estimated the animal to camera distance for 2,767 snapshot moments, consisting of 1,182 deer and 1,585 pigs.

### Automated Digital Data Processing
We uploaded 7,695 videos to Zamba. Using the European pretrained model, 638 videos contained deer, 836 contained pig, and 4,572 were blank. An additional 1,649 videos contained other objects.

### Automated Distance Estimation
We uploaded 7,189 snapshot moments and ran through Haucke's code (https://github.com/PJ-cs/DistanceEstimationTracking) to estimate distances from animals to the camera. A little more than 64% (4,631) of the snapshot moments were successfully processed and associated distance estimates were generated. Most of the 2,558 snapshot moments that failed to process were due to batches failing to run, distance estimates not being present in the output datafile, or negative distance estimates. Distances were estimated to 2,031 deer and 2,101 pigs using automated methods. Of the snapshot moments that failed, distances were estimated to 1,432 deer and 2,375 pigs using manual methods.

### Accuracy Statistics
Accuracy statistics for Zamba European model performance on our video dataset effectively identified deer and pigs for both north- and south-oriented videos (Table 1). Accuracy was > 80% for deer and pigs on both orientations, while precision and recall were > 90%. All objects achieved accuracy > 82% for north-oriented videos but was lower at 78% for south-oriented videos. The F1 score was above 0.9 for both orientations as well as the target species and all objects.

Table 1. Zamba model performance for detecting target species. Accuracy statistics are presented by camera orientation and for deer, pigs, and all objects. The number of videos (observations) in each category are provided.

| | North orientation | | | South orientation | | |
|---|---|---|---|---|---|---|
| Statistic | Deer | Pigs | All objects | Deer | Pigs | All objects |
| Accuracy | 83.1% | 84.2% | 82.7% | 81.6% | 80.5% | 78.2% |
| Precision | 95.8% | 93.2% | 92.7% | 92.1% | 92.1% | 94.4% |
| Recall | 94.8% | 96.1% | 94.2% | 91.0% | 87.7% | 90.1% |
| F1 | 0.95 | 0.95 | 0.93 | 0.92 | 0.90 | 0.92 |
| Number of observations | 792 | 779 | 944 | 473 | 507 | 684 |

We computed an accuracy assessment using 30 images where an animal was observed next to a reference flag staked out in 1-m intervals. We treated these distance measurements as truth. Automated distance estimates varied on average 1.07 m (SD 1.44 m) from our manual estimation of the distance (Appendix III). The automated procedure, in general, tended to place animals farther from the camera than their actual location.

**Period of Activity**

The percentage of time active varied little by species with estimated activity level for deer being 0.35 ± 0.01 (95% CI = 0.33–0.37), and for pigs being 0.35 ± 0.02 (95% CI = 0.32–0.39; Figure 3). These estimates were incorporated in the density estimator through a multiplier accounting for detection times, temporal availability with uncertainty, and the number of hours the cameras were operating per day. The CVs for the temporal availability estimates were small at 0.03 for deer and 0.06 for pigs. Deer showed a prominent peak between 04:00 and 06:00 hours (h), while deer activity was relatively low otherwise. During the two-hour peak activity period, there were 857 deer detections, which yield sufficient numbers to model PA Deer densities. For pigs, the peak at noon was isolated and surrounded by low activity levels. The single peak at 16:00 h was markedly different from the activity period between 18:00 and 21:00 h with a relatively low activity period at 17:00 h. However, to ensure adequate detections we used the period 16:00 to 21:00 h for modeling PA Pig densities. The respective datasets were subset to determine species-specific densities based on the peak activity periods.

**Density Estimation**

*All Deer density estimation*

There were 3,463 deer detections during the survey period, with 2,036 deer detections in the Plateau stratum and 1,427 deer detections in the Tarague stratum. Distances were left-truncated at 1 m, and distance bins of 1, 2, 3, 4, 5, 8, and 10 m were used as cutpoints in the All Deer analyses. Although hazard-rate and half-normal key models with cosine adjustment terms had the lowest AIC values, these models failed to converge during bootstrap procedures. The hazard-rate key model was chosen based on AIC accounting for overdispersion (Table 2). The chi-square goodness-of-fit tests were significant at the alpha = 0.05 level for both models, indicating the number of observations per bin differed from the expected value. Inspection of diagnostic plots also indicated that the model adequately fit the data with greatest deviations in the first two bins (Figure 4). The shoulder of the detection function extends out to 2 m before decaying rapidly. The estimated detection probability of a deer that was within 10 m of a camera was 0.136 (SE = 0.003; CV = 0.020).

Deer were more abundant in the Plateau stratum with a mean density of 0.54 deer/ha (95% CI = 0.18–1.05; CV = 0.43) than in the Tarague stratum with 0.49 deer/ha (95% CI 0.20–1.08; CV = 0.51; Table 3, Figure 5). Deer were more abundant in the Plateau stratum at 531 individuals (95% CI = 182–1,037) than in the Tarague stratum at 202 individuals (95% CI = 82–442). Total deer abundance was 733 individuals (95% CI = 296–1,359).

*Peak activity deer density estimation*

There were 1,193 deer detections during the two-hour peak activity period between 04:00 and 06:00 h, with 607 deer detections in the Plateau stratum and 586 deer detections in the Tarague stratum. Distance bins of 0, 1, 2, 3, 4, 5, 8, and 10 m were used as cutpoints in the PA Deer analyses. The half-normal key model with cosine adjustment terms had the lowest AIC value but failed to converge during bootstrap procedures. The half-normal key model was chosen based on AIC accounting for overdispersion (Table 4). The chi-square goodness-of-fit tests were

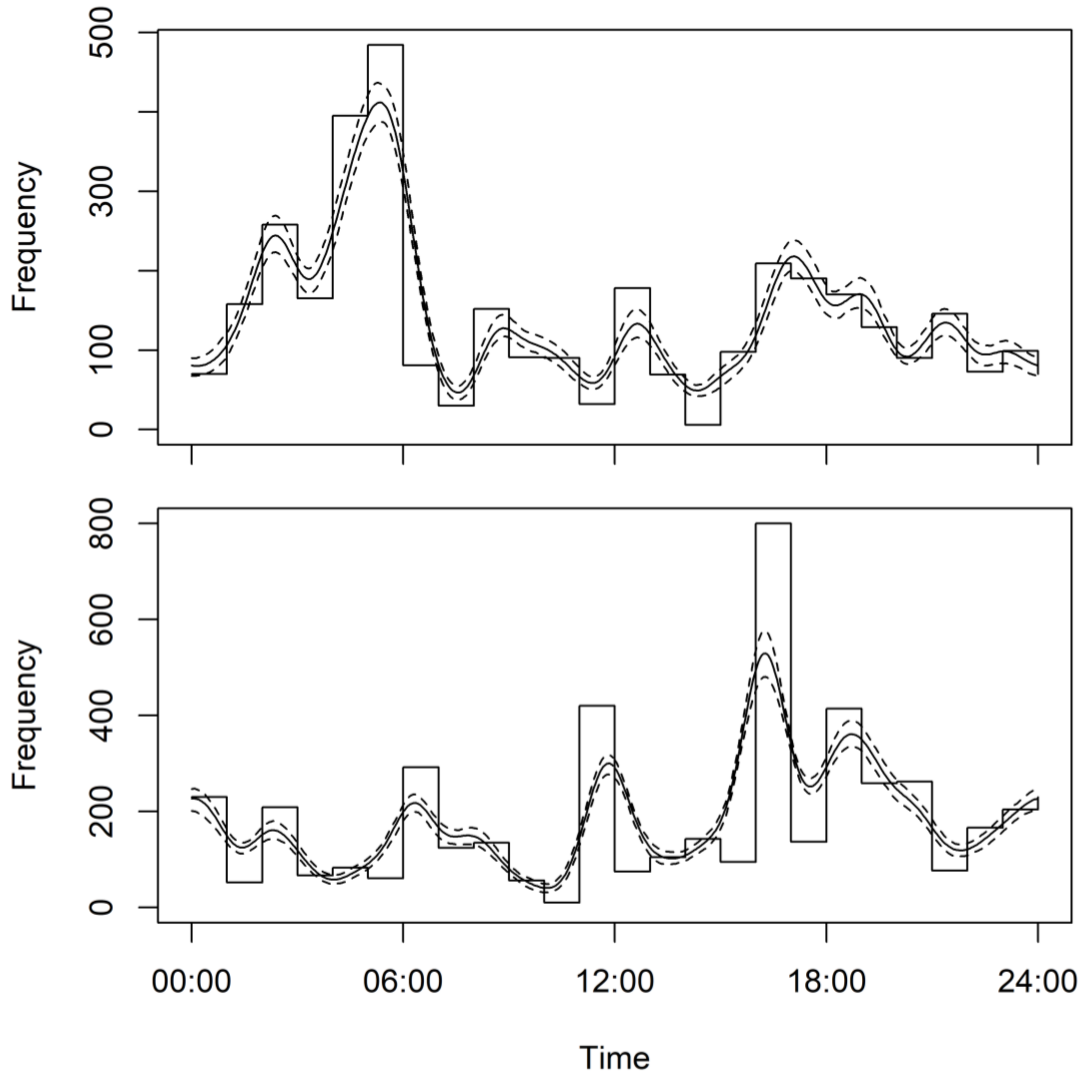


Figure 3. Activity patterns of deer (top panel) and pigs (bottom panel) from all camera trap records. Histograms are observed frequencies, and black curves are fitted circular kernel distributions with 95% CIs (confidence intervals; dashed curves).

Table 2. Detection function model selection statistics and parameter estimates for All Deer analyses. Key function with and without adjustment terms ranked by Akaike's information criterion (AIC) accounting for overdispersion ($\hat{c}$). Presented are the chi-square ($X^2$) goodness-of-fit statistic *p*-value, and the estimated average detection probability with standard error (SE).

| Key function | $X^2$ *p*-value | Average detectability | SE (Average detectability) | AIC | $\hat{c}$ |
|---|---|---|---|---|---|
| Hazard-rate | <0.001 | 0.136 | 0.003 | 10348.585 | 48.72 |
| Half-normal | <0.001 | 0.091 | 0.002 | 10398.447 | 76.83 |

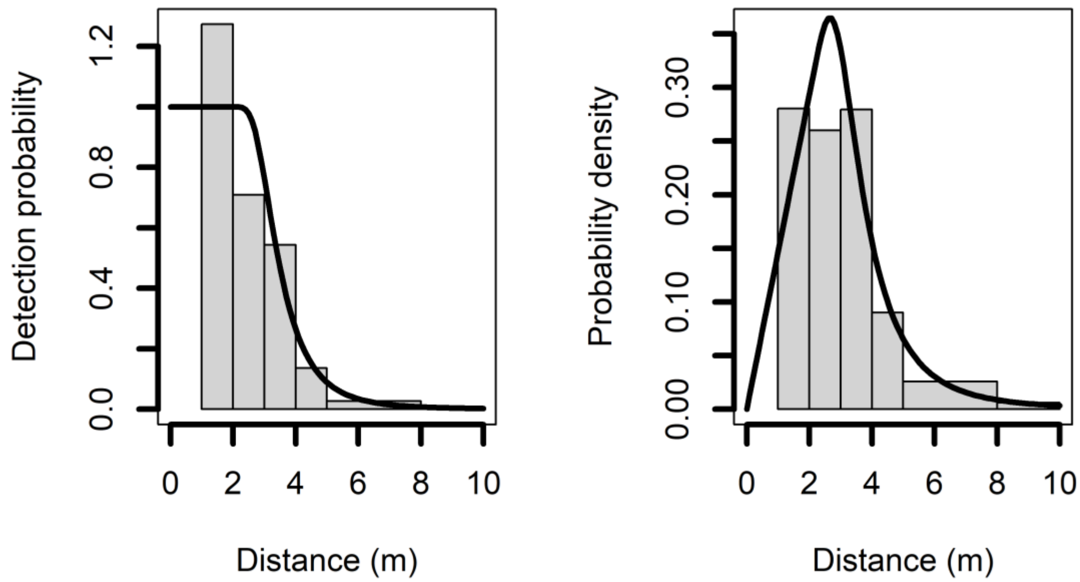


Figure 4. Detection function plots for the hazard-rate model without series expansion or covariates fitted to the All Deer detections. Plots represent the average detection probability (left panel) and probability density (right panel). There is moderate deviation in the histogram in the probability plots, which provides evidence that the function acceptably fits the data.

Table 3. All Deer estimates of median and mean densities (deer/ha; first row) and abundances (second row) with standard error (SE) for each stratum and total strata. Bootstrap derived 95% confidence intervals (lower limit = lcl; upper limit = ucl) are presented.

| Stratum | Median | Mean | SE | lcl | ucl |
|---|---|---|---|---|---|
| Plateau | 0.51 | 0.54 | 0.23 | 0.18 | 1.05 |
| | 501 | 531 | 229 | 182 | 1,037 |
| Tarague | 0.44 | 0.49 | 0.25 | 0.20 | 1.08 |
| | 182 | 202 | 101 | 82 | 442 |
| Total | 0.50 | 0.53 | 0.20 | 0.21 | 0.97 |
| | 695 | 733 | 286 | 296 | 1,359 |

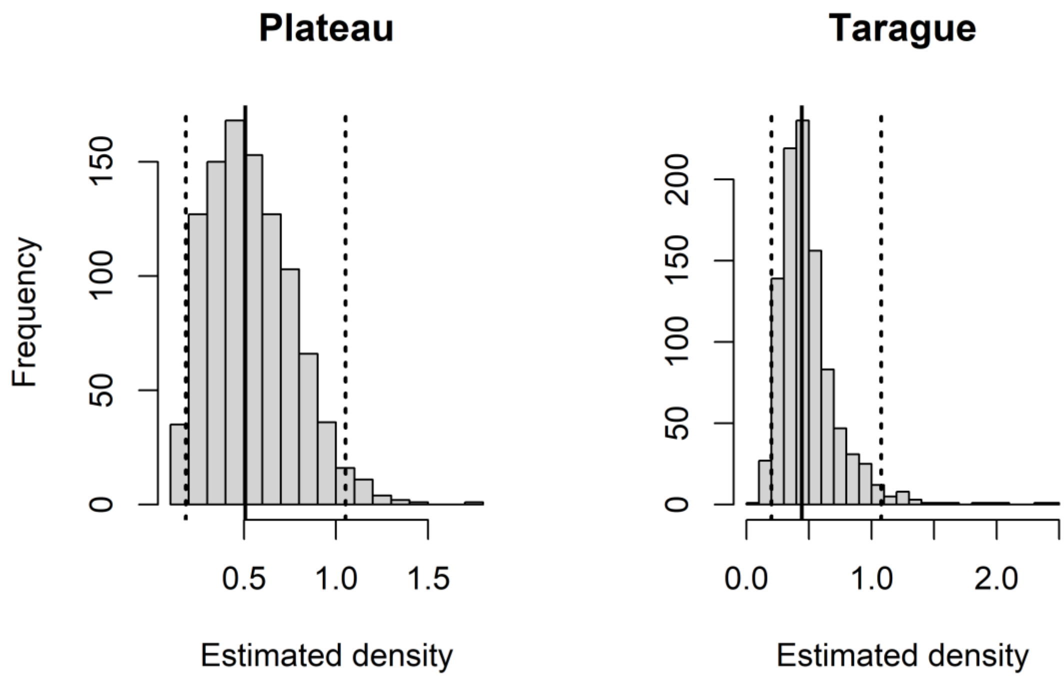


Figure 5. Median density estimates with 95% confidence intervals for All Deer by stratum (Plateau left panel and Tarague right panel) based on bootstrap procedures.

Table 4. Detection function model selection statistics and parameter estimates for deer detected during peak activity. Key function with and without adjustment terms ranked by Akaike's information criterion (AIC) accounting for overdispersion ($\hat{c}$). The chi-square ($X^2$) goodness-of-fit statistic and *p*-value and the estimated detection probability with standard error (SE) are presented.

| Key function | $X^2$ *p*-value | Average detectability | SE (Average detectability) | AIC | $\hat{c}$ |
|---|---|---|---|---|---|
| Half-normal | <0.001 | 0.106 | 0.003 | 3225.751 | 55.82 |
| Hazard-rate | <0.001 | 0.133 | 0.005 | 3287.906 | 88.15 |

significant at the alpha = 0.05 level for all models, indicating the number of observations per bin differed from the expected value. Inspection of diagnostic plots, however, indicated that the model adequately fit the data with greatest deviations in the first bin (Figure 6). The shoulder of the detection function extends a short distance before decaying rapidly. The estimated detection probability of a deer that was within 10 m of a camera was 0.105 (SE = 0.003; CV = 0.030).

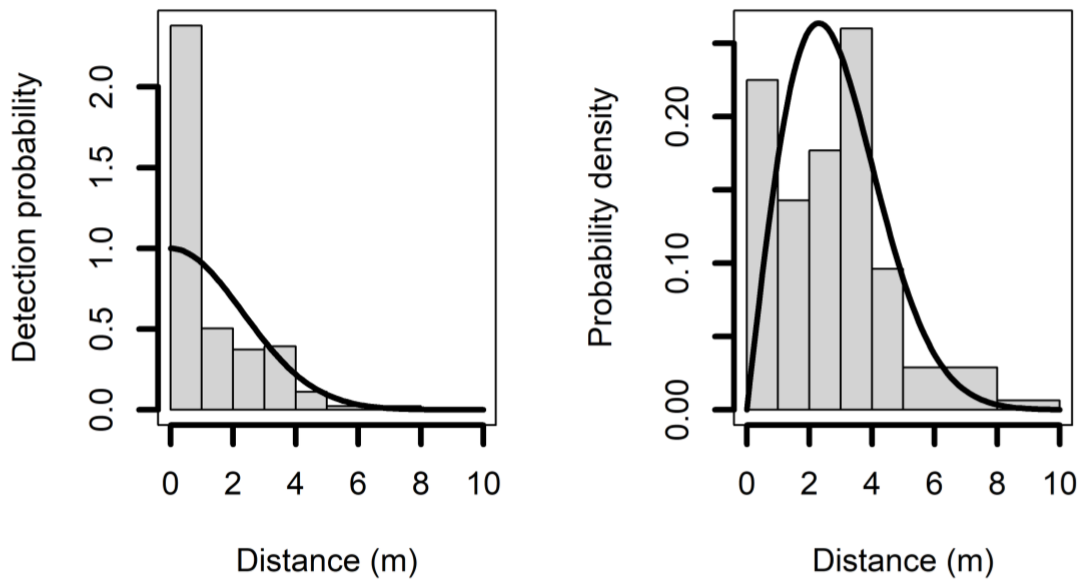


Figure 6. Detection function plots for the half-normal model without series expansion fitted to the PA Deer (deer during peak activity) detections. Plots represent the average detection probability (left panel) and probability density (right panel). There is moderate deviation in the histogram in the probability plots, which provides evidence that the function acceptably fits the data.

In contrast to the All Deer estimates, deer during the peak activity period had lower densities in the Plateau stratum with a mean density of 0.46 deer/ha (95% CI = 0.08–1.08; CV = 0.59) than in the Tarague stratum with 0.79 deer/ha (95% CI 0.11–2.07; CV = 0.67; Table 5, Figure 7). Due to the Plateau area being larger, deer were more abundant in the Plateau stratum at 431 individuals (95% CI = 71–1,011) than in the Tarague stratum at 326 individuals (95% CI = 45–849). Total deer abundance was 757 individuals (95% CI = 186–1,650).

Table 5. Median and mean density (deer/ha; first row) estimates of PA Deer (deer during peak activity) detections and abundances (second row) with standard error (SE) for each stratum and total strata. Bootstrap derived 95% confidence intervals (lower limit = lcl; upper limit = ucl) are presented.

| Stratum | Median | Mean | SE | lcl | ucl |
|---|---|---|---|---|---|
| Plateau | 0.42 | 0.46 | 0.27 | 0.08 | 1.08 |
| | 390 | 431 | 251 | 71 | 1,011 |
| Tarague | 0.68 | 0.79 | 0.53 | 0.11 | 2.07 |
| | 280 | 326 | 218 | 46 | 849 |
| Total | 0.53 | 0.56 | 0.28 | 0.14 | 1.22 |
| | 714 | 757 | 373 | 186 | 1,650 |

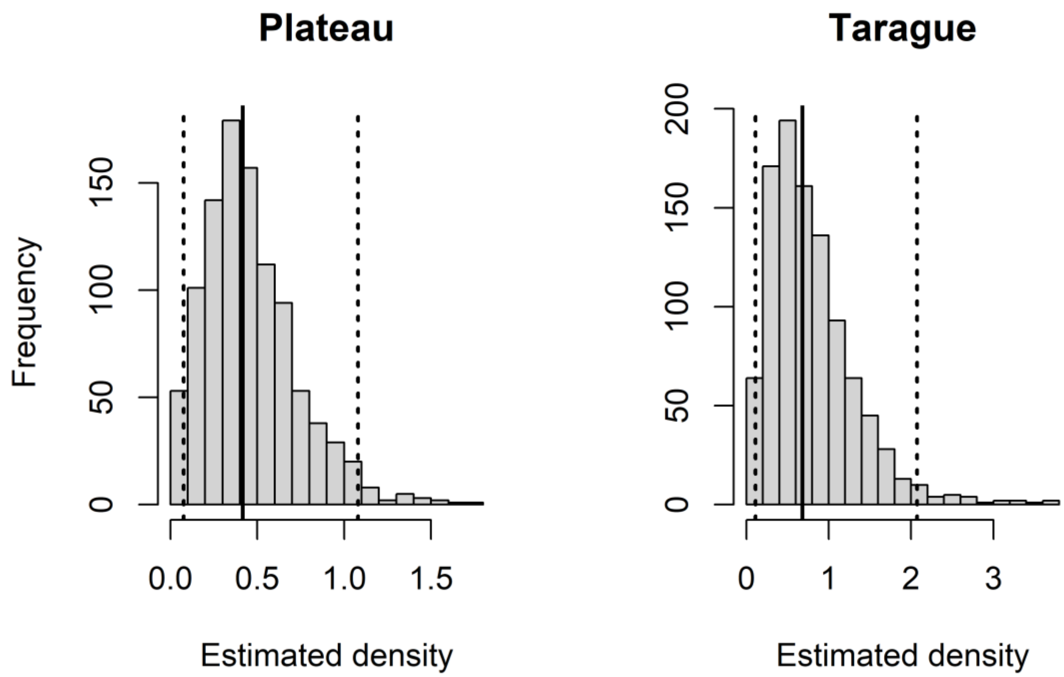


Figure 7. Median density estimates with 95% confidence intervals for PA Deer (deer during peak activity) detections by stratum (Plateau left panel and Tarague right panel) based on bootstrap procedures.

*All Pig density estimation*

There were 4,476 pig detections during the survey period, with 3,712 pigs detected in the Plateau stratum and 764 pigs detected in the Tarague stratum. The adjustment for temporal activity was 0.351 ± 0.017 (95% CI = 0.323–0.388). Distance bins of 0, 1, 2, 3, 4, 5, 8, and 10 m were used as cutpoints in the All Pig analyses. The hazard-rate key model was chosen based on AIC accounting for overdispersion (Table 6). The chi-square goodness-of-fit tests were significant at the alpha = 0.05 level for all models, indicating the number of observations per bin differed from the expected value. Inspection of diagnostic plots, however, indicated that the model adequately fit the data with greatest deviations in the first bin (Figure 8). The shoulder of the detection function extends out to 2 m before decaying rapidly. The estimated detection probability of a pig that was within 10 m of a camera was 0.222 (SE = 0.004; CV = 0.018).

Pigs were substantially more abundant in the Plateau stratum with a mean density of 0.66 pig/ha (95% CI = 0.21–1.73; CV = 0.58) than in the Tarague stratum with 0.20 pig/ha (95% CI 0.05–0.82; CV = 1.15; Table 7, Figure 9). Pigs were more abundant in the Plateau stratum at 654 individuals (95% CI = 211–1,708) than in the Tarague stratum at 82 individuals (95% CI = 19–338). Total pig abundance was 736 individuals (95% CI = 266–2,021).

Table 6. Detection function model selection statistics and parameter estimates for All Pigs. Key function with and without adjustment terms ranked by Akaike's information criterion (AIC) accounting for overdispersion ($\hat{c}$). The chi-square ($X^2$) goodness-of-fit statistic *p*-value and the estimated detection probability with standard error (SE) are presented.

| Key function | $X^2$ *p*-value | Average detectability | SE (Average detectability) | AIC | $\hat{c}$ |
|---|---|---|---|---|---|
| Hazard-rate | <0.001 | 0.222 | 0.004 | 16263.93 | 127.46 |
| Hazard-rate + cos | <0.001 | 0.187 | 0.007 | 16232.29 | 143.16 |
| Half-normal | <0.001 | 0.163 | 0.002 | 16497.55 | 143.20 |

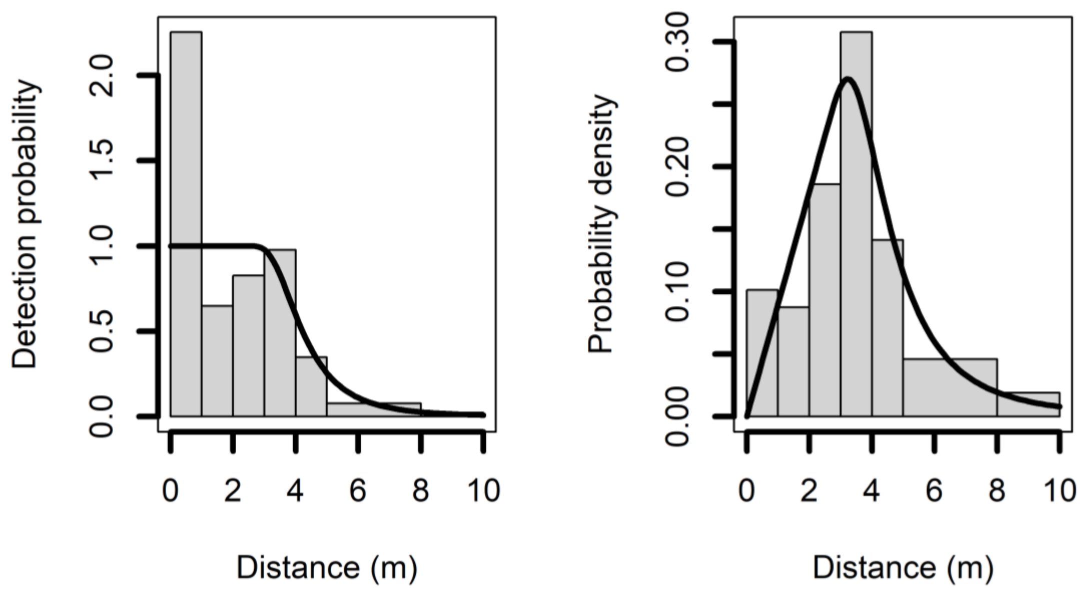


Figure 8. Detection function plots for the hazard-rate model without series expansion fitted to the All Pig detections. Plots represent the average detection probability (left panel) and probability density (right panel). There is moderate deviation in the histogram in the probability plots, which provides evidence that the function acceptably fits the data.

Table 7. All Pig estimates of median and mean densities (pig/ha; first row) and abundances (second row) with standard error (SE) for each stratum and total strata. Bootstrap derived 95% confidence intervals (lower limit = lcl; upper limit = ucl) are presented.

| Stratum | Median | Mean | SE | lcl | ucl |
|---|---|---|---|---|---|
| Plateau | 0.59 | 0.66 | 0.38 | 0.21 | 1.73 |
| | 584 | 654 | 376 | 211 | 1,708 |
| Tarague | 0.15 | 0.20 | 0.23 | 0.05 | 0.82 |
| | 60 | 82 | 94 | 19 | 338 |
| Total | 0.47 | 0.53 | 0.32 | 0.19 | 1.45 |
| | 651 | 736 | 446 | 266 | 2,021 |

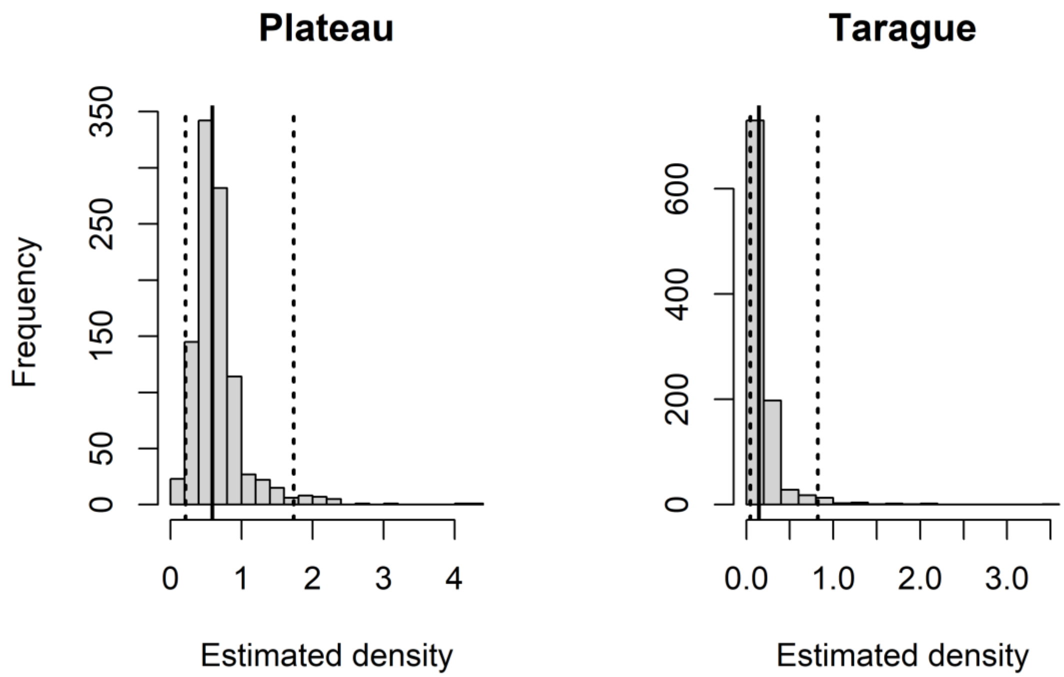


Figure 9. Median density estimates with 95% confidence intervals for All Pigs by stratum (Plateau left panel and Tarague right panel) based on bootstrap procedures.

*Peak activity pig density estimation*

There were 1,859 pig detections during the five-hour peak activity period between 16:00 and 21:00 h, with 1,495 pigs detected in the Plateau stratum and 364 pigs detected in the Tarague stratum. Distances were left-truncated at 1 m and distance bins of 1, 2, 3, 4, 5, 8, and 10 m were used as cutpoints in the PA Pig analyses. The hazard-rate key model was chosen based on AIC accounting for overdispersion (Table 8). The chi-square goodness-of-fit tests were significant at the alpha = 0.05 level for all models, indicating the number of observations per bin differed from the expected value. Inspection of diagnostic plots, however, indicated that the model adequately fit the data with greatest deviations in the first bin (Figure 10). The shoulder of the detection function extends to about 3 m before decaying rapidly. The estimated detection probability of a pig that was within 10 m of a camera was 0.138 (SE = 0.003; CV = 0.022).

Table 8. Detection function model selection statistics and parameter estimates for pigs detected during peak activity. Key function with and without adjustment terms ranked by Akaike's information criterion (AIC) accounting for overdispersion ($\hat{c}$). Presented are the chi-square ($X^2$) goodness-of-fit statistic *p*-value and the estimated detection probability with standard error (SE).

| Key function | $X^2$ *p*-value | Average detectability | SE (Average detectability) | AIC | $\hat{c}$ |
|---|---|---|---|---|---|
| Half-normal | <0.001 | 0.138 | 0.003 | 7073.603 | 121.51 |
| Hazard-rate | <0.001 | 0.193 | 0.005 | 6977.399 | 137.67 |

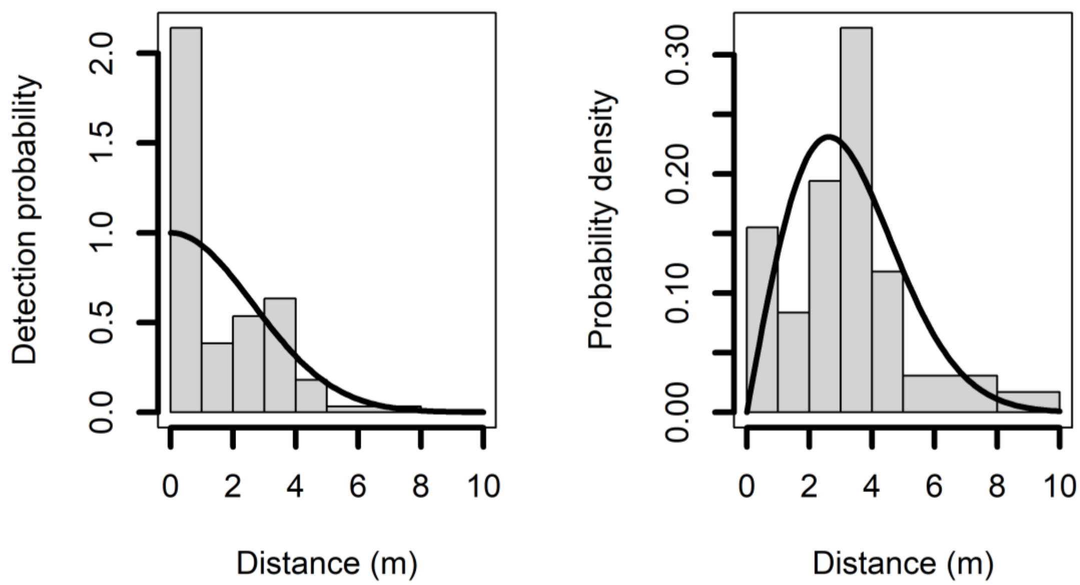


Figure 10. Detection function plots for the half-normal model without series expansion fitted to the PA Pig (pig peak activity) detections. Plots represent the average detection probability (left panel) and probability density (right panel). There is moderate deviation in the histogram in the probability plots, which provides evidence that the function acceptably fits the data.

Pigs during the peak activity period had higher densities in the Plateau stratum with a mean density of 0.55 pigs/ha (95% CI = 0.11–1.25; CV = 0.55) than in the Tarague stratum with 0.17 pigs/ha (95% CI 0.03–0.41; CV = 0.59; Table 9, Figure 11). Pigs were more abundant in the Plateau stratum at 518 individuals (95% CI = 101–1,172) than in the Tarague stratum at 71 individuals (95% CI = 14–169). Total pig abundance was 589 individuals (95% CI = 156–1,258).

Table 9. Median and mean density of pigs (pigs/ha; first row) and abundances (second row) detected during peak activity with standard error (SE) for each stratum and total strata. Bootstrap derived 95% confidence intervals (lower limit = lcl; upper limit = ucl) are presented.

| Stratum | Median | Mean | SE | lcl | ucl |
|---|---|---|---|---|---|
| Plateau | 0.52 | 0.55 | 0.30 | 0.11 | 1.25 |
| | 482 | 518 | 280 | 101 | 1,172 |
| Tarague | 0.16 | 0.17 | 0.10 | 0.03 | 0.41 |
| | 64 | 71 | 41 | 14 | 169 |
| Total | 0.42 | 0.44 | 0.22 | 0.12 | 0.95 |
| | 553 | 589 | 289 | 156 | 1,258 |

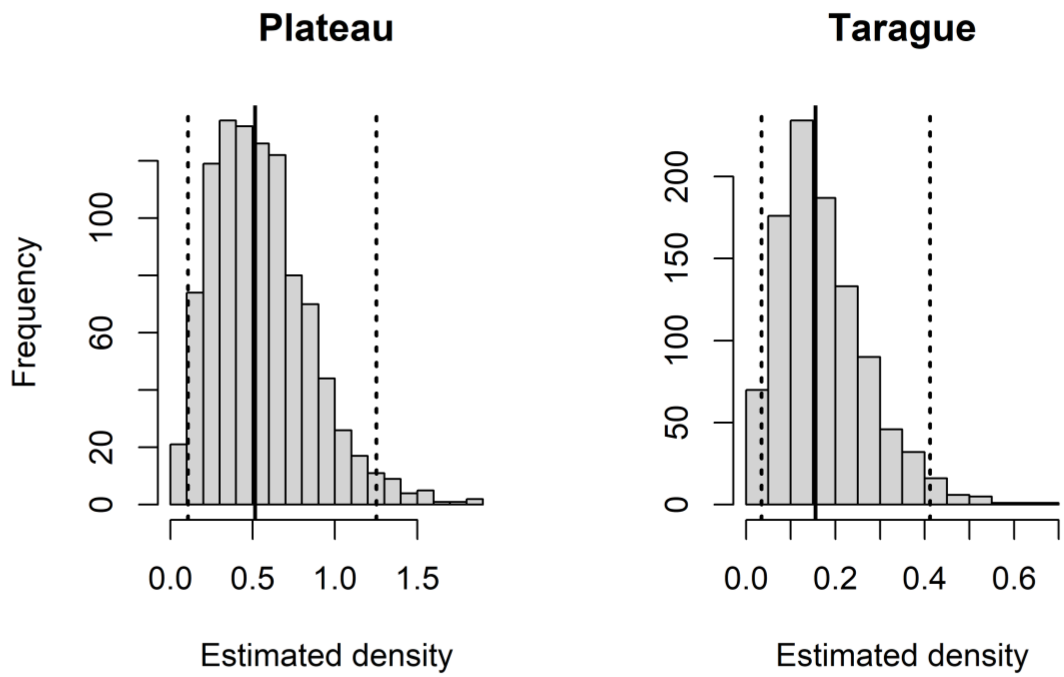


Figure 11. Median density estimates with 95% confidence intervals for PA Pig (pig peak activity) detections by stratum (Plateau left panel and Tarague right panel) based on bootstrap procedures.

**Adequate Coverage**

The number of camera trap points required to achieve the target CV values of 0.10, 0.20, 0.30, and 0.40 varied by species and if using estimates for all the data or only data from peak activity periods. The CVs ranged from 0.38 to 1.15 (mean = 0.59 ± 0.19), and estimates of deer densities were more precise in general (i.e., had smaller CVs) than estimates of pig densities (Table 10). Deer estimates were more precise using all detections than data from just peak activity periods. In contrast, pig densities were more precise for the peak activity period than using all detections. In general, precision increased with increasing sampling effort where CVs were largest for estimates in Tarague stratum and lowest for the combined total strata. The CVs in the Plateau stratum typically fell between the Tarague stratum and combined total strata rather than closer to one or the other. The number of camera traps required to obtain desired CVs of 0.10 was substantial, ranging from a 14.2- to 132.3-fold increase in camera traps. Estimates with CVs of 0.20 were more achievable, ranging from a 3.6- to 33.1-fold increase in camera traps. Doubling to quadrupling the number of camera traps would yield CVs of 0.30, except in Tarague for All Pigs which would require a 14.7-fold increase. Increasing the number of camera traps slightly, ranging from current levels to doubling the effort, would achieve CVs of 0.40, except in Tarague for All Pigs that would require an 8.3-fold increase.

Table 10. Coefficients of variation (CV), number of detections (n), and number of camera traps deployed ($K_0$) to achieve desired CVs of 0.10, 0.20, 0.30, and 0.40 ($K_{est}$) for deer and pigs by stratum. Estimates were computed for All and PA (peak activity) datasets separately.

| Species | Stratum | CV | n | $K_0$ | $K_{0.1}$ | $K_{0.2}$ | $K_{0.3}$ | $K_{0.4}$ |
|---|---|---|---|---|---|---|---|---|
| All | | | | | | | | |
| Deer | Plateau | 0.43 | 2,036 | 26 | 472 | 118 | 52 | 29 |
| | Tarague | 0.51 | 1,427 | 12 | 312 | 78 | 35 | 20 |
| | Total | 0.38 | 3,463 | 38 | 541 | 135 | 60 | 34 |
| Pigs | Plateau | 0.58 | 3,712 | 26 | 862 | 215 | 96 | 54 |
| | Tarague | 1.15 | 764 | 12 | 1,587 | 397 | 176 | 99 |
| | Total | 0.60 | 4,476 | 38 | 1,385 | 346 | 154 | 87 |
| PA | | | | | | | | |
| Deer | Plateau | 0.59 | 1,742 | 26 | 896 | 224 | 100 | 56 |
| | Tarague | 0.67 | 968 | 12 | 540 | 135 | 60 | 34 |
| | Total | 0.50 | 2,678 | 38 | 950 | 238 | 106 | 59 |
| Pigs | Plateau | 0.55 | 1,742 | 26 | 774 | 193 | 86 | 48 |
| | Tarague | 0.59 | 968 | 12 | 415 | 104 | 46 | 26 |
| | Total | 0.50 | 2,678 | 38 | 950 | 238 | 106 | 59 |

**Trapping Effort**

On average, 101.9 ± 82.3 deer were detected per day with a range of 0 to 263 detections. Sampling at least three days should provide a minimum number of deer detections to reliably model the deer detection function. On average, 131.6 ± 118.8 pigs were detected per day with a range of 0 to 432 detections. Sampling at least two days should provide a minimum number of detections to reliably model the pig detection function. Many more trap days would be needed if fewer than 30 camera traps are deployed.

The daily deer detection rate decreased between the first and eighth days and then increased steadily through the remaining days (Figure 12, top row, left panel). Each additional trap day yielded an average increase of 0.029 deer detections. Breakpoints occurred just after trap days 3, 10, 18, and 26 (psi scores = 3.46, 10.61, 18.28, and 26.21). A post-hoc assessment of daily detection rate, dropping the first trap day, possessed breakpoints on similar days, and the daily detection rate increased by an average of 0.034 deer detections (Figure 12, top row, right panel).

Pig daily detection rate increased steadily during the first 10 days where a breakpoint was identified (psi score = 9.89) and leveled off through the remaining trap days (Figure 12, middle row, left panel). Each additional trap day yielded an average increase of 0.039 pig detections. Trap days 1, 2, and 15 were outliers, but only trap day 2 was outside the Cook’s distance in the residuals versus leverage plot. A post-hoc assessment of daily detection rate, dropping the first trap day, yielded a breakpoint near day 10 (psi score = 9.90), and the daily detection rate increased by an average of 0.035 pig detections (Figure 12, middle row, right panel).

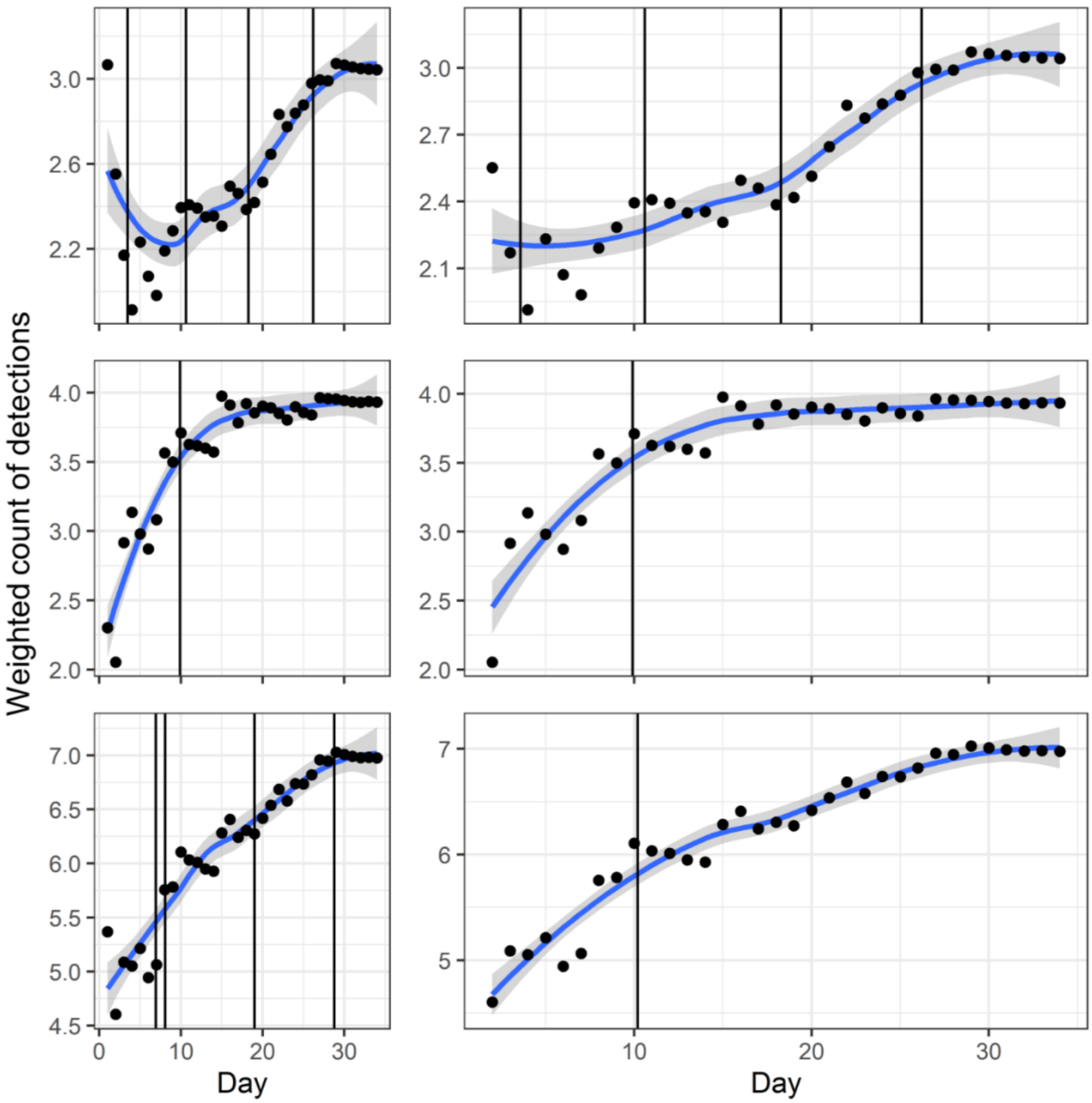


Figure 12. Weighted daily detections (black circles) of deer (top row), pigs (middle row), and both detections combined (bottom row). Panels in the left column include the first trap day detections, while panels in the right column exclude the first trap day detections. The blue lines are the loess smooth fitted to the daily number of detections, weighted by cumulative trap days, and the ribbons are the 95% confidence intervals. The vertical lines identify breakpoints.

The combined deer and pig daily number of detections, weighted by cumulative trap days, increased throughout the trapping period with breakpoints on days 6, 8, 19, and 28 (psi scores = 6.93, 8.09, 19.00, and 28.79; Figure 12, bottom row, left panel). Each additional trap day yielded an average increase of 0.068 combined deer and pig detections. Trap days 2, 6, and 34 were outliers for the combined deer and pig daily detection rates. However, no trap days were outside the Cook's distance in the residuals versus leverage plot. A post-hoc assessment of the combined deer and pig daily detection rate, dropping the first trap day, yielded a breakpoint near day 10 (psi score = 10.19), and the daily detection rate increased by an average of 0.069 combined deer and pig detections (Figure 12, bottom row, right panel).

**Microsite Heterogeneity**

Individual camera orientation density estimates were generally less precise for deer and pigs than estimates made from the full datasets. Differences in the north-oriented deer CV estimates were generally larger than CVs estimated from the full dataset (range = -0.058–0.210). All south-oriented deer CVs were larger than the full dataset CVs (range = 0.094–0.209). For pigs, the differences in CVs compared to the full dataset estimates were larger for north-oriented detections (range = 0.611–0.750) than for south-oriented detections (range = 0.003–0.058) and the magnitude difference varied by strata. CVs were least different for total strata and most different for the Tarague stratum estimates in all comparisons, except for the north-oriented, Tarague stratum CV which was the only CV that was more precise than the full dataset CVs.

## DISCUSSION

We developed a camera trap survey design based on standard camera trap sampling protocols using motion-activated, digital cameras and determined that distance sampling methods using camera traps produce reliable densities of unmarked deer and pigs on Guam. To facilitate processing large amounts of video images, we developed an imagery processing pipeline using an automated machine learning algorithm for species detection and identification, and a separate automated machine learning algorithm to estimate distances from each detected animal to the camera. We fitted detection functions to these distances to estimate detection probabilities accounting for imperfect detection and estimated densities using design-based methods.

Overall, our study-wide density estimates were 0.53 deer/ha (95% CI = 0.21–0.97) and 0.53 pigs/ha (95% CI = 0.19–1.45). Our deer estimate was substantially lower than the Wiles *et al.* (1999) estimate of 6–8 deer/ha in the AAFB Munitions Storage Area (MSA), based on extrapolation of nighttime spotlight counts, although there is some doubt about the estimator validity. Our density estimates were slightly lower than those of Knutson and Vogt (2002) who sampled in the MSA and estimated densities of 1.8 deer/ha (95% CI = 1.4–2.2) based on drive count methods. Our lower estimates could be due to depredation management and hunting pressures in the Plateau stratum and depredation management in the Tarague stratum. We were not able to resample in the MSA, an area where ungulates are controlled by MSA staff.

Our stratum-specific deer densities were similar to each other at 0.54 and 0.49 deer/ha in the Plateau and Tarague strata, respectively. Sundance-EA (2020) estimated 1–2 deer/ha in fenced areas where ungulates had been eradicated, which was roughly two to four times larger than our Tarague estimate. Differences in our density estimates with those of Sundance-EA (2020) could be due to intensive depredation management efforts where 1,379 deer were removed from both strata in 2021 and 2022, and with more females removed than males (1:0.72 female to male ratio; M. Burt, NAVFACMAR, written communication, 28 February 2023). Within a 33-ha fenced area in Tarague, 15 deer were removed, which is a density of 0.45 deer/ha and corroborates our estimate (M. Burt, NAVFACMAR, written communication, 28 February 2023). Within the North Finegayan Forest Enhancement Sites, Sundance-EA (2022) estimated 2–3 deer/ha, an area that had not previously received depredation management or ungulate control. Their densities are comparable to estimates of Knutson and Vogt (2002) and Sundance-EA (2020) before depredation management was enacted in the Plateau and Tarague strata. Thus, due to reductions in deer through control efforts, it is likely that CTDS did not underestimate deer in our study area.

Our total strata and Plateau stratum pig densities (0.66 pigs/ha; 95% CI = 0.21–1.73) were very similar to Knutson and Vogt's (2002) estimate of 0.4 pigs/ha (95% CI = 0.2–0.6), Sundance-EA's (2020) estimate of 0.5 pigs/ha, and Sundance-EA's (2022) estimate of 0.48 pigs/ha. Our pig estimate for the Tarague stratum (0.20 pigs/ha; 95% CI = 0.05–0.82) was substantially lower than the estimate by Sundance-EA (2020). Our generally lower estimate could be due to the estimator being negatively biased, but more likely is due to depredation management and control pressures in the Tarague stratum where 206 pigs were removed in 2021 and 2022, and with more females removed than males (1:0.79 female to male ratio; M. Burt, NAVFACMAR, written communication, 28 February 2023). In a 33-ha fenced area in Tarague, 55 pigs were removed, yielding a density of 1.67 pigs/ha. There was reproduction in the pig population during the year it took to eradicate pigs, which may explain why their estimates were higher (M. Burt, NAVFACMAR, written communication, 28 February 2023). Our uncertainty was relatively large with CVs ranging from 0.38 to 1.15 (Table 10), and the 95% CIs bracketed published point estimates. Our camera trap survey design is based on a regularly sized trapping grid that is generalizable, can be scaled to accommodate additional camera traps to minimize estimator uncertainty, and can be expanded to survey deer and pigs in other areas of AAFB as well as elsewhere on Guam.

**Considerations for Future Sampling**

Our camera trap survey design provides adequate sampling to meet the objective to estimate densities and track trends of both deer and pigs simultaneously. Sampling at more locations, either by sampling all grid points in the Plateau stratum on the 500- x 500-m regular grid or sampling on a higher-density regular grid would be required to achieve desired CVs. Moreover, increasing the number of camera trap sites and sampling for longer periods of time may be necessary if populations decline, whether by recreational hunting, management to control and eradicate ungulates in areas of high conservation value, or other biotic or abiotic conditions. To reduce the required number of cameras to sample all points on a high-density grid, Palencia *et al.* (2021) noted that using a moving survey approach where camera traps are deployed in one subset of the grid (e.g., every other point) and then moved to a new location (e.g., the remaining points) will increase the sampled locations and increase precision. Below, we note several points to consider for future deer and pig sampling to monitor populations, and in Appendix IV we provide best practices for expanding the study design to new areas.

*Availability*

We suggest using all the video imagery to estimate species-specific densities instead of sub-setting the dataset to the peak activity period and estimate temporal availability to account for conditions specific to each study and minimize estimator bias. The synchrony assumption is relaxed a bit through restricting inference to individuals in the sampled population during peak activity period. Not accounting for the proportion of active animals can positively bias density estimates; however, narrowly defining peak activity periods to when a large majority of animals are active can minimize such bias. The proportion of animals active throughout the sampling period can be included in the denominator of the density estimator equation (Howe *et al.* 2017), thus using all of the data and minimizing small sample size issues (e.g., where few animals are detected during narrowly defined peak activity periods). Alternatively, Rowcliffe *et al.* (2014) assumes that activity level is the only determinant of the rate at which camera traps detect animals, then the trap rate is proportional to the level of activity and the amount of activity is proportional to the area under the trap rate curve. Rowcliffe *et al.* (2014) estimates the trap rate curve using circular probability density functions. Estimates of activity level standard error can be derived from nonparametric bootstrapping methods sampling the data with replacement and refitting the model. Densities can then be adjusted by the proportion of time when animals are available along with its uncertainty (Howe *et al.* 2017, Nakashima *et al.* 2018).

Importantly, regardless of whether temporal availability or peak activity is used, the availability metric should be estimated for each specific camera trap study (Appendix I). We observed differences in the peak activity periods among three camera trap studies, indicating that species- and location-specific temporal availability or peak activity should be estimated specific to each study to avoid availability bias.

*Sampling period*

Deer and pig detectability likely changes between the dry and wet seasons. The sampling period for deer and pigs would require sampling during both the dry and wet season, thus the cameras need to be able to withstand tropical rainy season conditions. Seasonal changes in activity and movement patterns within the area sampled would benefit from investigation to account for seasonally variable detectability and peak activity periods.

*Solar time*

Peak activity is usually tuned to sunrise or sunset, which can have a strong influence at high latitudes resulting in overestimating activity levels (Nouvellet *et al.* 2012, Rowcliffe *et al.* 2014). Nouvellet *et al.* (2012) developed methods to translate local clock time into solar time based on latitude and date at which photographs were taken. Effects of solar time are minimized near the equator, and the time of sunrise and sunset on Guam is relatively stable. If the effect of solar time is deemed a concern, the equations and code from Nouvellet *et al.* (2012) can be used to translate local clock time to solar time to evaluate the need to produce activity-level estimates accounting for solar time.

*Adequate coverage*

Guidance on determining spacing among camera traps for CTDS methods is limited, but in general spacing is relatively flexible. In contrast, spacing among camera traps based on mark-recapture and occupancy methods require between site independence, with the distance between camera traps either based on the smallest home range of the target species or close enough to catch the same individuals at more than one location (Gilbert *et al.* 2021). Most uncertainty in CTDS population estimates is derived from the encounter rate variation due to the small size of the area monitored at a camera trap site (Howe *et al.* 2019, Cappelle *et al.* 2021). A high-density grid better captures the heterogeneity among trap sites than a low-density grid leading to reduced encounter rate variation and more precise abundance estimates. An alternative approach to using a high-density grid to capture heterogeneity among trap sites is to move cameras to new locations in proximity of the trap site, say within 10 m, or rotate the orientation of each camera on a low-density grid. Rotating camera orientation will likely be more efficient than finding new suitable trees, and rotation can be accomplished when visiting the trap sites to replace batteries and SD cards during the survey. Another approach would be to increase the number of cameras deployed at each point to provide greater coverage, which should help to achieve target CVs. There are differences in the numbers of detections and estimator certainty between the north and south oriented cameras, a result of microsite heterogeneity. Therefore, having two cameras at each trap point should increase sample sizes, capture microsite heterogeneity, and produce estimates with narrower confidence intervals.

Greater numbers of camera traps would be needed for pigs than deer to achieve desired CVs. Incorporating a high-density grid providing greater coverage would be necessary to achieve CVs of 0.2 and 0.3. However, authors in many multi-species studies conclude that optimizing camera trap spacing for certain species either over- or under-samples for others (e.g., Foster and Harmsen 2012, Hofmeester *et al.* 2019, Gilbert *et al.* 2021). Differences have been attributed to temporal activity levels and availability, directionality and speed of movement, and resource availability. The behavior of both deer and pigs on Guam are likely similar enough to not require species-specific sampling designs. However, optimal species-specific spacing and density may be needed when species reach low densities.

*Trapping effort*

Buckland *et al.* (2015) recommends fitting detection functions with at least 75 to 100 detections for point-transect distance sampling and extended methods. A minimum number of deer detections to reliably model the detection function was achieved after three sampling days, while sufficient pig detections were achieved after two sampling days. Post-hoc assessments of daily detection rate showed that deer detections increased throughout the sampling period while the pig daily detection rate increased until about day 10 before leveling off. The combined deer and pig daily detection rate yielded a breakpoint near day 10. Sampling for about two weeks would optimize collecting during the period where daily detection rates increased the most for both deer and pigs.

We followed recommendations by Howe *et al.* (2017) to drop detections made on the day cameras were deployed and retrieved. However, the detection rates on the first day post deployment were outliers in daily deer and pig detections. Trap sites may be avoided the first few days after deployment but dropping only the deployment day data may not be sufficient to minimize estimator bias (Palencia *et al.* 2021).

Martin *et al.* (2017) found that moisture accumulation on camera trap sensors resulted in 25% of the camera units failing during the wet season that had worked during the dry season. This was despite using professional, top-quality cameras that had been prepared for tropical conditions that were similar to conditions and equipment used on Guam. Therefore, equipment failure or malfunction may require cameras be replaced, or more cameras may need to be deployed and for a longer period to ensure adequate coverage of the study area and record the minimum number of detections to reliably model the detection probability.

*Microsite and orientation*

Hofmeester *et al.* (2019) showed that microsite conditions influence animal detection and concluded that these factors are probably most important for camera trap sampling. Due in part to smaller sample sizes, we expected the north and south CV estimates to be slightly less precise than CVs estimated from the full datasets, on the order of 10 to 20% larger, if there was minimal microsite variability. This was the case for deer where north- and south-oriented CVs differed by < 0.21 from the full dataset CVs. Of note, the north-oriented, Tarague stratum estimates were the only estimates that were more precise than estimates from the full dataset. The deer population is relatively large in the study area, and deer are readily captured at camera traps providing sufficient detections to reliably estimate detection probabilities. The north-oriented and full dataset pig CVs were markedly different with north-oriented CVs being generally twice that of the full dataset CVs. Differences in the south and full dataset pig CVs were small with CVs differing by < 0.06 and well within our expected 10 to 20% difference.

In addition to varying microsite conditions, the length of sampling may influence estimator CVs. The north-oriented cameras were deployed on average 14 days (± 10.4 days) while the south-oriented cameras collected data for an average of only two more days than north-oriented cameras (16 ± 8.6 days). However, nearly twice as many deer and almost four times as many pigs were detected when cameras were oriented south (2,082 and 3,031, respectively) than detected when cameras were oriented north (1,176 and 783, respectively). Schaus *et al.* (2020), Kays *et al.* (2021), and Palencia *et al.* (2021) recommend increasing the number of camera traps, generally by maximizing the number of locations sampled. Differences between north and south CV comparisons indicate that deer and pigs may not be moving uniformly throughout trap sites. Increasing coverage by sampling additional orientations, such as sampling the four cardinal directions, will likely yield larger gains in estimator precision than gains achieved from increasing the number of trap locations. In addition, standardizing the length of time cameras are deployed in any given orientation likely would minimize this source of variability and permit greater microsite sampling.

*Camera placement*

Note that many camera trap studies preferentially set trap locations to sample on well-established trails for convenience because dense vegetation can channel animal movements through trails and for fear of no or few detections (Harmsen *et al.* 2010, Palencia *et al.* 2021). Fonteyn *et al.* (2020) explored the effect of placing camera traps subjectively and oriented their cameras so the FOV included wildlife trails or deployed using more robust systematic sampling design with a predefined density of traps on regularly spaced grids. Kolowski and Forrester (2017) also explored the effect of camera trap placement and orientation with respect to trails and other features. Both studies found that camera trap placement did not strongly influence the detection probabilities for most species, but Kolowski and Forrester (2017) showed that the white-tailed deer (*Odocoileus virginianus*) detection probabilities were higher on game trails, and neither study looked for differences in pigs. In practice, the limitation of a lower detection probability can be countered by a longer sampling period. Several biotic (e.g., animal activity patterns, movement, and body size) and abiotic (e.g., terrain, vegetative density, and weather conditions) factors influence the detection process, which are controlled for by randomized designs and imperfect species detection estimated using CTDS.

*Empirical AOV versus manual FOV*

Differences in the empirical AOV and the FOV listed in the camera manufacturer's manual can differ by 10 degrees or more, which can bias low density estimates (Corlatti *et al.* 2020). To account for obstructions, such as vegetation and cliff faces, and edge-effects, a best practice approach is to measure the FOV for each camera to minimize this bias.

*Estimator bias*

Estimates may be biased when animals move and are not detected at their original locations (Buckland *et al.* 2015). We observed animals seemingly being spooked by the cameras triggering and moving quickly out of the FOV. Animals that reacted to the camera being triggered did so within the triggering period and first second of recording. These detections were thus discarded using our approach in defining snapshot moments; thus, minimizing bias. This approach was also used by Bessone *et al.* (2020), although Palencia *et al.* (2021) noted that this approach may not solve the reactive animal bias issue. In addition, bias can occur when animals close to the camera block the view of distant animals, although this was not an issue in our study.

*Automated digital data processing*

Our use of Zamba for object detection and identification led to a large reduction in processing time while maintaining sufficient levels of accuracy. We also found the user experience of uploading videos to the Zamba website and having DrivenData processing on the backend to be fluid, easy to use, and efficient. Upload time was manageable for our needs; taking 40 minutes to upload 100 videos of 11MB each. Processing digital data through the Zamba website allows research teams with minimal programming experience to utilize cutting-edge machine learning algorithms. In contrast, running the Zamba application locally for object detection and identification would expedite processing efficiencies and require a research team member with Python programming experience.

We found that the European model version 2.1.0 performed well on our dataset (Table 1). This is despite the model being trained on a different background from our study site and indicates the model is generalizing well across different backgrounds. Our target species aligned well with species in the European model, which may have contributed to the high model accuracy. Future studies would likely benefit from running machine learning algorithms that were trained on animals similar to the animals in their dataset. Overall, the ability of Zamba to classify a large portion of our videos (69%) led to large decreases in manual processing time and will likely lead to similar time savings for future studies.

*Automated distance processing*

Using automated distance estimation methods helped estimate distances for a large number of animals, but the high processing failure rate (36%) required manually estimating distances to more than 2,000 snapshot moment images. Reasons for failures included batches failing to run, distance estimates not being generated for all images uploaded (e.g., 400 images were uploaded but distance estimates only came back for 300), and negative distance estimates being generated. Given the failure rate, this led to substantial amounts of manual processing, and we did not observe a significant reduction in processing time for this task.

Nonetheless, automated distance estimation holds great promise. Some of the issues may have been due to how we processed the images. We uploaded images to process on a cloud-based coding environment rather than running the script locally, which is likely to be more stable and have fewer processing failures. Additionally, distance estimation code is rapidly developing and improving (Haucke *et al.* 2022, Johanns *et al.* 2022), and future iterations of the code may mitigate some of the issues we had. Automated distance estimation is a top priority for the field of machine learning CTDS, and several teams are developing automated distance estimation algorithms (e.g., DrivenData). As such, more stable and efficient automated distance estimation algorithms may be available for future CTDS studies.

## ACKNOWLEDGEMENTS

Editorial and online publishing support provided by Sarah Nash through the Hawaiʻi Cooperative Studies Unit. Funding was provided by the U.S. Navy (Commander, Navy Installation Command, NAVFAC Marianas) grant #N4155721MP001GE and U.S. Geological Survey Invasive Species Program. We thank Matt Burt and Scott Vogt, natural resources specialists, AAFB Guam, for information on deer and pigs on Guam, providing the Moultrie cameras, and assistance with access to the base, study design, camera deployment, reorientation, retrieval, processing the digital imagery, and review of a draft report. We thank Matt Kedziora, natural resources specialist, NAVFACMAR, Navy Base Guam, for providing the 14 Bushnell Trophy cameras. Mike Park, natural resources specialist, AAFB Guam, assisted with camera deployment, reorientation, and retrieval. The data analyzed in this study are available on request from NAVFACMAR. This was an observational study; thus, no animals were handled in accordance with animal welfare standards of the Institutional Animal Care and Use Committee.

## LITERATURE CITED

Amidon, F., M. Metevier, and S. E. Miller. 2017. Vegetation mapping of the Mariana Islands: Commonwealth of the Northern Mariana Islands and the Territory of Guam: Final report. U.S. Fish and Wildlife Service, Pacific Islands Fish and Wildlife Office, and Pacific Islands Climate Change Cooperative, Honolulu, Hawaiʻi, USA.

Amstrup, S. C., T. L. McDonald, and B. F. J. Manly, editors. 2005. Handbook of capture-recapture analysis. Princeton University Press, Princeton, New Jersey, USA.

Beery, S., D. Morris, and S. Yang. 2019. Efficient pipeline for camera trap image review. arXiv preprint arXiv:1907.06772.

Bessone, M., H. S. Kühl, G. Hohmann, I. Herbinger, K. P. N'Goran, P. Asanzi, P. B. Da Costa, V. Dérozier, E. D. B. Fotsing, B. I. Beka, M. D. Iyomi, I. B. Iyatshi, P. Kafando, M. A. Kambere, D. B. Moundzoho, M. L. K. Wanzalire, and B. Fruth. 2020. Drawn out of the shadows: surveying secretive forest species with camera trap distance sampling. Journal of Applied Ecology 57:963–974.

Buckland, S. T. 2006. Point transect surveys for songbirds: robust methodologies. The Auk 123:345–357.

Buckland, S. T., D. R. Anderson, K. P. Burnham, J. L. Laake, D. L. Borchers, and L. Thomas. 2001. Introduction to distance sampling: estimating abundance of biological populations. Oxford University Press, Oxford, UK.

Buckland, S. T., D. R. Anderson, K. P. Burnham, J. L. Laake, D. L. Borchers, and L. Thomas. 2004. Advanced distance sampling: estimating abundance of biological populations. Oxford University Press, Oxford, UK.

Buckland, S. T., E. A. Rextad, T. A. Marques, and C. S. Oedekoven. 2015. Distance sampling: methods and applications. Springer, London, UK.

Burnham, K. P., and D. R. Anderson. 2002. Model selection and multimodel inference: A practical information-theoretic approach, second edition. Springer-Verlag, New York, New York, USA.

Camp, R. J., M. H. Reynolds, B. L. Woodworth, P. M. Gorresen, and T. K. Pratt. 2009. Monitoring Hawaiian forest birds. Pages 83–107 *in* T. K. Pratt, C. T. Atkinson, P. C. Banko, J. D. Jacobi, and B. L. Woodworth (editors). Conservation biology of Hawaiian forest birds: implications for insular avifauna. Yale University Press, New Haven, Connecticut, USA.

Cappelle, N., E. J. Howe, C. Boesch, and H. S. Kühl. 2021. Estimating animal abundance and effort–precision relationship with camera trap distance sampling. Ecosphere 12:e03299.

Cappelle, N., M. Després-Einspenner, E. J. Howe, C. Boesch, and H. S. Kühl. 2019. Validating camera trap distance sampling for chimpanzees. American Journal of Primatology 81:e22962.

Caron, M., H. Touvron, I. Misra, H. Jégou, J. Mairal, P. Bojanowski, and A. Joulin. 2021. Emerging properties in self-supervised vision transformers. Pages 9650–9660 *in* Proceedings of the IEEE/CVF international conference on computer vision.

Chandler, R. B., and J. A. Royle. 2013. Spatially explicit models for inference about density in unmarked or partially marked populations. The Annals of Applied Statistics 7:936–954.

Choiński, M., M. Rogowski, P. Tynecki, D. P. J. Kuijper, M. Churski, and J. W. Bubnicki. 2021. A first step towards automated species recognition from camera trap images of mammals using AI in a European temperate forest. Pages 299–310 *in* K. Saeed and J. Dvorský (editors). Computer information systems and industrial management. Springer International Publishing, London, UK. https://doi.org/10.1007/978-3-030-84340-3_24

Conry, P. J. 1988. Management of feral and exotic game species on Guam. Transactions of the Western Section of the Wildlife Society 24:26–30.

Corlatti, L., S. Sivieri, B. Sudolska, S. Giacomelli, and L. Pedrotti. 2020. A field test of unconventional camera trap distance sampling to estimate abundance of marmot populations. Wildlife Biology 2020(4):wlb.00652. https://doi.org/10.2981/wlb.00652

ENETWILD-consortium, P. Acevedo, S. Croft, G. Smith, J. A. Blanco-Aguiar, J. Fernandez-Lopez, M. Scandura, M. Apollonio, E. Ferroglio, O. Keuling, M. Sange, S. Zanet, F. Brivio, T. Podgórski, K. Petrović, R. Soriguer and J. Vicente. 2019. ENETwild modelling of wild boar distribution and abundance: update of occurrence and hunting data-based models. EFSA supporting publication 2019:EN-1674. 29 pp. https://doi.org/10.2903/sp.efsa.2019.EN-1674

Evans, B. E., C. E. Mosby, and A. Mortelliti. 2019. Assessing arrays of multiple trail cameras to detect North American mammals. PLoSONE 14(6):e0217543. https://doi.org/10.1371/journal.pone.0217543

Evans, M. J., and T. A. G. Rittenhouse. 2018. Evaluating spatially explicit density estimates of unmarked wildlife detected by remote cameras. Journal of Applied Ecology 55:2565–2574.

Facil, J. M., B. Ummenhofer, H. Zhou, L. Montesano, T. Brox, and J. Civera. 2019. CAM-Convs: Camera-aware multi-scale convolutions for single-view depth. Pages 11826–11835 *in* Proceedings of the IEEE/CVF Conference on Computer Vision and Pattern Recognition.

Fennell, M., C. Beirne, and A. C. Burton. 2022. Use of object detection in camera trap image identification: assessing a method to rapidly and accurately classify human and animal detections for research and application in recreation ecology. Global Ecology and Conservation 35:e02104. https://doi.org/10.1016/j.gecco.2022.e02104

Fewster, R. M., S. T. Buckland, K. P. Burnham, D. L. Borchers, P. E. Jupp, J. L. Laake, and L. Thomas. 2009. Estimating the encounter rate variance in distance sampling. Biometrics 65:225–236.

Fonteyn, D., C. Vermeulen, N. Deflandre, D. Cornelis, S. Lhiest, F. G. A. Houngbegnon, J.-L. Doucet, and A. Fayolle. 2020. Wildlife trail or systematic? Camera trap placement has little effect on estimates of mammal diversity in a tropical forest in Gabon. Remote Sensing in Ecology and Conservation. https://doi.org/10.1002/rse2.191

Foster R. J., and B. J. Harmsen. 2012. A critique of density estimation from camera-trap data. The Journal of Wildlife Management 76:224–236.

Ghazoul, J., and S. Sheil. 2010. Tropical rain forest ecology. Oxford University Press, Oxford, UK.

Gilbert, N. A., J. D. J. Clare, J. L. Stenglein, and B. Zuckerberg. 2021. Abundance estimation of unmarked animals based on camera-trap data. Conservation Biology 35:88–100.

Harmsen, B. J., R. J. Foster, S. Silver, L. Ostro, and C. P. Doncaster. 2010. Differential use of trails by forest mammals and the implications for camera-trap studies: a case study from Belize. Biotropica 42:126–133.

Harris, G. M., M. J. Butler, D. R. Stewart, E. M. Rominger, and C. Q. Ruhl. 2020. Accurate population estimation of Caprinae using camera traps and distance sampling. Scientific Reports 10:17729.

Haucke, T., H. S. Kühl, J. Hoyer, and V. Steinhage. 2022. Overcoming the distance estimation bottleneck in camera trap distance sampling. arXiv:2105.04244v1.

Haucke, T., and V. Steinhage. 2021. Exploiting depth information for wildlife monitoring. arXiv:2102.05607v1.

Hess, S. C., N. H. Wehr, and C. M. Litton. 2020. Wild pigs in the Pacific islands. Pages 403–421 *in* K. C. Vercauteren, J. C. Beasley, S. S. Ditchkoff, J. J. Mayer, G. J. Roloff, and B. K.

Strickland (editors). Invasive wild pigs in North America: ecology, impacts, and management. CRC Press: Taylor and Francis Group, Boca Raton, Florida, USA.

Hofmeester, T. R., J. M. Rowcliffe, and P. A. Jansen. 2017. A simple method for estimating the effective detection distance of camera traps. Remote Sensing in Ecology and Conservation 3:81–89.

Hofmeester, T. R., J. P. G. M. Cromsigt, J. Odden, H. Andrén, J. Kindberg, and J. D. C. Linnell. 2019. Framing pictures: a conceptual framework to identify and correct for biases in detection probability of camera traps enabling multi-species comparison. Ecology and Evolution 9:2320–2336.

Hoiem, D., A. A. Efros, and M. Hebert. 2005. Automatic photo pop-up. ACM Transactions on Graphics 24:577–584. https://doi.org/10.1145/1073204.1073232

Howe, E. J., S. T. Buckland, M.-L. Despres-Einspenner, and H. S. Kühl. 2017. Distance sampling with camera traps. Methods in Ecology and Evolution 8:1558–1565.

Howe, E. J., S. T. Buckland, M.-L. Despres-Einspenner, and H. S. Kühl. 2019. Model selection with overdispersed distance sampling data. Methods in Ecology and Evolution 10:38–47.

Johanns, P., T. Haucke, and V. Steinhage. 2022. Automated distance estimation for wildlife camera trapping. Ecological Informatics 70:101734.

JRMNRS. 2012. Draft Joint Region Marianas; Andersen Air Force Base ungulate management plan. Guam: Joint Region Marianas Integrated Natural Resources Management Plan, U.S. Navy, 70.

Kays, R., A. Hody, D. S. Jachowski, and A. W. Parsons. 2021. Empirical evaluation of the spatial scale and detection process of camera trap surveys. Movement Ecology 9:41.

Kays, R., B. S. Arbogast, M. Baker-Whatton, C. Beirne, H. M. Boone, M. Bowler, S. F. Burneo, B. V. Cove, P. Ding, S. Espinosa, A. L. S. Concalves, C. P. Hansen, P. A. Jansen, J. M. Kolowski, T. W. Knowles, M. G. M. Lima, J. Millspaugh, W. J. McShea, K. Pacifici, A. W. Parsons, B. S. Pease, F. Rovero, F. Santos, S. G. Schuttler, D. Sheil, X. Si, M. Snider, and W. R. Spironello. 2020. An empirical evaluation of camera trap study design: how many, how long and when? Methods in Ecology and Evolution 11:700–713.

Kelly, M. 2008. Design, evaluate, refine: Camera trap studies for elusive species. Animal Conservation 11:182–184.

Kéry, M., and J. A. Royle. 2016. Applied hierarchical modeling in ecology. Volume 1. Elsevier, London, UK.

Knutson, K., and S. Vogt. 2002. Philippine deer (*Cervus mariannus*) and feral pig (*Sus scrofa*) population sampling in the secondary limestone forest of northern Guam. Prepared for Naval Facilities Marianas by Andersen Air Force Base, Guam, USA.

Kolowski, J. M., and T. D. Forrester. 2017. Camera trap placement and the potential for bias due to trails and other features. PLoS ONE 12:e0186679. https://doi.org/10.1371/journal.pone.0186679

Krizhevsky, A., I. Sutskever, and G. E. Hinton. 2012. Imagenet classification with deep convolutional neural networks. Communications of the ACM 60:84–90.

Lander, M. A., and C. P. Guard. 2003. Creation of a 50-year rainfall database, annual rainfall climatology, and annual rainfall distribution map for Guam: Mangilao, Guam. University of Guam, Water and Environmental Research Institute. Technical Report No. 102, 20 pp. plus appendices.

Link, W. A., M. R. Schofield, R. J. Barker, and J. R. Sauer. 2018. On the robustness of N-mixture models. Ecology 99:1547–1551.

Lucas, T. C. D., E. A. Moorcroft, R. Freeman, J. M. Rowcliffe, and K. E. Jones. 2015. A generalised random encounter model for estimating animal density with remote sensor data. Methods in Ecology and Evolution 6:500–509.

Marques, F. F. C., and S. T. Buckland. 2004. Covariate models for the detection function. Pages 31-47 *in* S. T. Buckland, D. R. Anderson, K. P. Burnham, J. L. Laake, D. L. Borchers, and L. Thomas (editors). Advanced distance sampling: estimating abundance of biological populations. Oxford University Press, Oxford, UK.

Martin, E. H., V. G. Ndibalema, and F. Rovero. 2017. Does variation between dry and wet seasons affect tropical mammals' occupancy and detectability by camera traps? Case study from the Udzungwa Mountains, Tanzania. African Journal of Ecology 55:37–46.

Miller, D. L., E. A. Rexstad, L. Thomas, L. Marshall, and J. L. Laake. 2019. Distance sampling in R. Journal of Statistical Software 89:1–28.

Moeller, A. K., P. M. Lukacs, and J. S. Horne. 2018. Three novel methods to estimate abundance of unmarked animals using remote cameras. Ecosphere 9:e02331.

Muggeo, V. M. R. 2022. Segmented: regression models with break-points/change-points (with possible random effects) estimation, version 1.6-2. The Comprehensive R Archive Network (CRAN).

Nakashima, Y., K. Fukasawa, and H. Samejima. 2018. Estimating animal density without individual recognition using information derivable exclusively from camera traps. Journal of Applied Ecology 55:735–744. https://doi.org/10.1111/1365-2664.13059.

Nouvellet, P., G. S. Rasmussen, D. W. Macdonald, and F. Courchamp. 2012. Noisy clocks and silent sunrises: measurement methods of daily activity pattern. Journal of Zoology 286:179–184.

Pal, R., T. Bhattacharya, Q. Qureshi, S. T. Buckland, and S. Sathykumar. 2021. Using distance sampling with camera traps to estimate the density of group-living and solitary mountain ungulates. Oryx 55:668–676.

Palencia, P., J. M. Rowcliffe, J. Vicente, and P. Acevedo. 2021. Assessing the camera trap methodologies used to estimate density of unmarked populations. Journal of Applied Ecology. https://doi.org/10.1111/1365-2664.13913

Parsons, A. W., T. Forrester, W. J. McShea, M. C. Baker-Whatton, J. J. Millspaugh, and R. Kays. 2017. Do occupancy or detection rates from camera traps reflect deer density? Journal of Mammalogy 98:1547–1557.

Pollock, K. H., J. D. Nichols, T. R. Simons, G. L. Farnsworth, L. L. Bailey, and J. R. Sauer. 2002. Large scale wildlife monitoring studies: statistical methods for design and analysis. Environmetrics 13:105–119.

Primack, R., and R. Corlett. 2005. Tropical rain forests: an ecological and biogeographical comparison. Blackwell Publishing, Malden, Massachusetts, USA.

R Core Team. 2021. R: a language and environment for statistical computing. Version 4.2.1. R Foundation for Statistical Computing, Vienna, Austria.

Rovero, F., E. Martin, M. Rosa, J. A. Ahumada, and D. Spitale. 2014. Estimating species richness and modelling habitat preferences of tropical forest mammals from camera trap data. PLoS One 9:e0118330.

Rovero, F., and F. Zimmermann. 2016. Camera trapping for wildlife research. Pelagic Publishing Ltd.

Rowcliffe, J. M. 2021. Activity: Animal activity statistics. R package version 1.3.1.

Rowcliffe, J. M., C. Carbone, P. A. Jansen, R. Kays, and B. Kranstauber. 2011. Quantifying the sensitivity of camera traps using an adapted distance sampling approach. Methods in Ecology and Evolution 2:467–476.

Rowcliffe, J. M., J. Field, S. T. Turvey, and C. Carbone. 2008. Estimating animal density using camera traps without the need for individual recognition. Journal of Applied Ecology 45:1228–1236.

Rowcliffe, J. M., R. Kays, B. Kranstauber, C. Carbone, and P. A. Jansen. 2014. Quantifying levels of animal activity using camera trap data. Methods in Ecology and Evolution 5:1170–1179.

Royle, J. A., and J. D. Nichols. 2003. Estimating abundance from re-peated presence-absence data or point counts. Ecology 84:777–790.

Royle, J. A., R. B. Chandler, R. Sollmann, and B. Gardner. 2014. Spatial capture-recapture. Academic Press, Waltham, Massachusetts, USA.

Saxena, A., M. Sun, and A. Y. Ng. 2009. Make3d: Learning 3d scene structure from a single still image. IEEE Transactions on Pattern Analysis and Machine Intelligence 31:824–840.

Schaus, J., A. Uzal, L. K. Gentle, P. J. Baker, L. Bearman-Brown, S. Bullion, A. Gazzard, H. Lockwood, A. North, T. Reader, D. M. Scott, C. S. Sutherland, and R. W. Yarnell. 2020. Application of the random encounter model in citizen science projects to monitor animal densities. Remote Sensing in Ecology and Conservation 6:514–528.

Si, X., R. Kays, and P. Ding. 2014. How long is enough to detect terrestrial animals? Estimating the minimum trapping effort on camera traps. PeerJ 2:e374.

Sollmann, R., A. Mohamed, H. Samejima, and A. Wilting. 2013. Risky business or simple solution—relative abundance indices from camera-trapping. Biological Conservation 159:405–412.

Steenweg, R., M. Hebblewhite, R. Kays, J. Ahumada, J. T. Fisher, C. Burton, S. E. Townsend, C. Carbone, J. M. Rowcliffe, J. Whittington, J. Brodie, J. A. Royle, A. Switalski, A. P. Clevenger, N. Heim, and L. N. Rich. 2017. Scaling-up camera traps: monitoring the planet's biodiversity with networks of remote sensors. Frontiers in Ecology and the Environment 15:26–34.

Sundance-EA Associates Joint Venture. 2020. Construction of ungulate (deer and pig) fence at Naval Support activity Andersen Base: final ungulate density survey results. Prepared for Naval Facilities Marianas by Sundance-EA Associates Joint Venture, Barrigada, Guam, USA.

Sundance-EA Associates Joint Venture. 2022. Final feral ungulate removal for forest enhancement sites at Naval Computer and Telecommunications Station and Andersen Air Force Base, Northern Guam. Prepared for Naval Facilities Marianas by Sundance-EA Associates Joint Venture, Barrigada, Guam, USA.

Tabak, M. A., M. S. Norouzzadeh, D. W. Wolfson, S. J. Sweeney, K. C. Vercauteren, N. P. Snow, J. M. Halseth, P. A. Di Salvo, J. S. Lewis, M. D. White, B. Teton, J. C. Beasley, P. E. Schlichting, R. K. Boughton, B. Wight, E. S. Newkirk, J. S. Ivan, E. A. Odell, R. K. Brook, P. M. Lukacs, A. K. Moeller, E. G. Mandeville, J. Clune, and R. S. Miller. 2019.

Machine learning to classify animal species in camera trap images: applications in ecology. Methods in Ecology and Evolution 10:585–590.

Tan, M., W. Chao, J.-K. Cheng, M. Zhou, Y. Ma, X. Jiang, J. Ge, L. Yu, and L. Feng. 2022. Animal detection and classification from camera trap images using different mainstream object detection architectures. Animals 12, article 15. https://doi.org/10.3390/ani12151976

Thomas, L., S. T. Buckland, E. A. Rexstad, J. L. Laake, S. Strindberg, S. L. Hedley, J. R. B. Bishop, T. A. Marques, and K. P. Burnham. 2010. Distance software: design and analysis of distance sampling surveys for estimating population size. Journal of Applied Ecology 47:5–14. https://doi.org/10.1111/j.1365-2664.2009.01737.x

Tribble, G., J. Stock, and J. Jacobi. 2016. Watershed processes from ridge to reef: consequences of feral ungulates for coral reef and effects of watershed management. Page 194 *in* C. E. Stringer, K. W. Krauss, and J. S. Latimer (editors). Headwaters to estuaries: advances in watershed science and management. Proceedings of the Fifth Interagency Conference on Research in the Watersheds. USDA. March 2–5, 2015, North Charleston, South Carolina, USA.

Wiles, G. J. 2012. *Rusa marianna* (Philippine deer). *In* CABI Compendium. Wallingford, UK: CAB International. https://doi.org/10.1079/cabicompendium.89935 (accessed on 12 November 2021).

Wiles, G. J., D. W. Buden, and D. J. Worthington. 1999. History of introduction, population status, and management of Philippine deer (*Cervus mariannus*) on Micronesian islands. Mammalia 63:193–215.

Young, S., J. Rode-Margono, and R. Amin. 2018. Software to facilitate and streamline camera trap data management: A review. Ecology and Evolution 8:9947–9957.

Zou, K. H., A. J. O'Malley, and L. Mauri. 2007. Receiver-operating characteristic analysis for evaluating diagnostic tests and predictive models. Circulation 115:654–657.

## APPENDIX I: TEMPORAL AVAILABILITY

We analyzed previously collected still shot images to determine if deer and pig availability differ among study areas and times. We accounted for species availability by sub-setting the dataset for distance sampling to determine species-specific peak activity periods. Activity level was estimated using the R package *activity* (Rowcliffe 2021). The time stamp (24:00 clock; hh:mm) for each occurrence was converted to radian time using the *gettime()* function. The level of activity was modeled with the *fitact()* function and 95% confidence intervals were estimated from bootstrap procedures with 999 iterations. Peak activity levels were compared both within and between species using the *compareTime()* function. Finally, we performed a randomization test to determine the probability that two sets (deer and pigs) of circular observations come from the same distribution using the *compareCkern()* function and 999 iterations.

Peak activity level for deer and pigs was determined from the Naval Munitions Station Fence #1 trail camera data collected over a two-week period in June and July 2021. During the first week, four camera traps were in a Vitex mixed native forest above a cliff line and set for eight nights. The second week, four camera traps were in coconut/native mixed forest below the cliff line and set for seven nights. Each camera was set to collect video, except for one camera in the first week that collected still shot photos. This camera was reset to collect video for seven nights, and the still shot photos were not used in this study. Camera traps were mounted securely to trees 30–35 cm above the ground and programmed using default setting to trigger and record a still shot photo. A total of 67 trap nights were sampled yielding 59 occurrences of 1 to 2 deer detected (mean = 1.1, SD = 0.3) and 66 occurrences of 1 to 5 pigs detected (mean = 2.0, SD = 1.3). Activity level was determined using methods described above.

In the Naval Munitions Station Fence #1 trail camera data, deer were most active early in the morning with a minor activity period near dusk, whereas pigs were most active late morning through dusk, with a peak just before dusk (Appendix I, Figure 1). For deer, there were no differences within the two peak activity periods, and there was no difference between the two activity periods (Wald statistic = 0.86, $p = 0.35$). The peak pig activity around 17:30 h was not different from the extended activity period (using 12:00 h as reference; Wald statistic = 2.21, $p = 0.14$); however, pig activity between 16:00 and 17:30 h was significantly different (Wald statistic = 5.85, $p = 0.02$).

The overlap between the two species kernel distributions was low (0.30), the index of overlap was low (0.21), and the difference in the deer and pig activity level estimates was significant (Wald statistic = 5.59, $p = 0.02$). This was supported by the randomization test where there was no evidence that the two sets came from the same distribution ($p < 0.001$). From a practical perspective, species-specific peak activity periods should be used to avoid bias. The sampling period for deer should include detections from just the early morning four-hour peak activity period (03:00 to 07:00 h). For pigs, an extended sampling period is appropriate from 09:00 to 18:00 h, although there is evidence to truncate the pig activity period before the initial dip at 15:00 h. Therefore, the sampling period for pigs should include detections from the six-hour peak activity period (09:00 to 15:00 h).

A second camera trap study was conducted in the Tarague area following the methods for the NMS Fence #1 study. Peak activity levels were different in the Tarague camera trap study (Appendix I, Figure 2). The index of overlap was moderate (0.57), and the deer and pig activity level estimates overlapped substantially (Wald statistic = 0.98, $p = 0.32$). However, most of the overlap occurred between 17:00 to 22:00 h with an overlapping peak near dawn (06:00 h). The randomization test revealed that there was no evidence that the two sets came from the same distribution ($p < 0.001$). This was due to differences in activity levels in early morning and

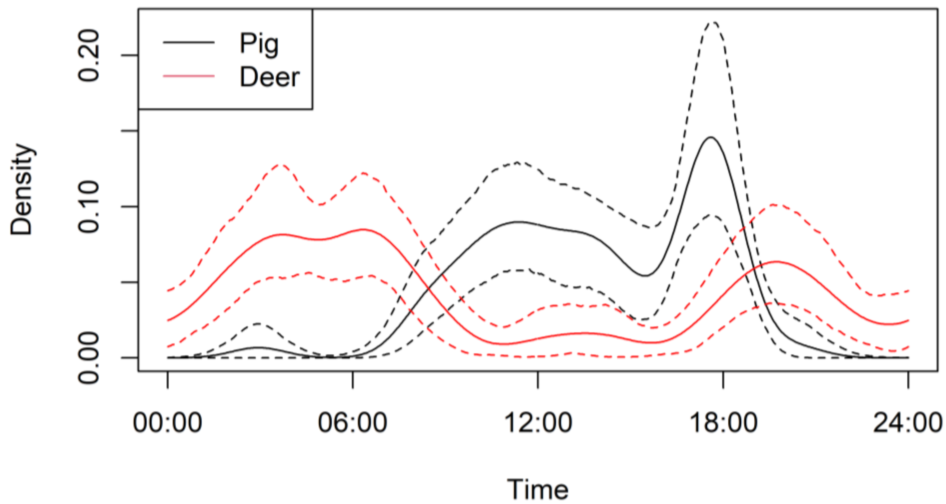


Appendix I, Figure 1. Activity level for pigs (black) and deer (red) from Naval Munitions Station Fence #1 trail camera trap data. Dotted lines are 95% confidence intervals computed from bootstrap methods.

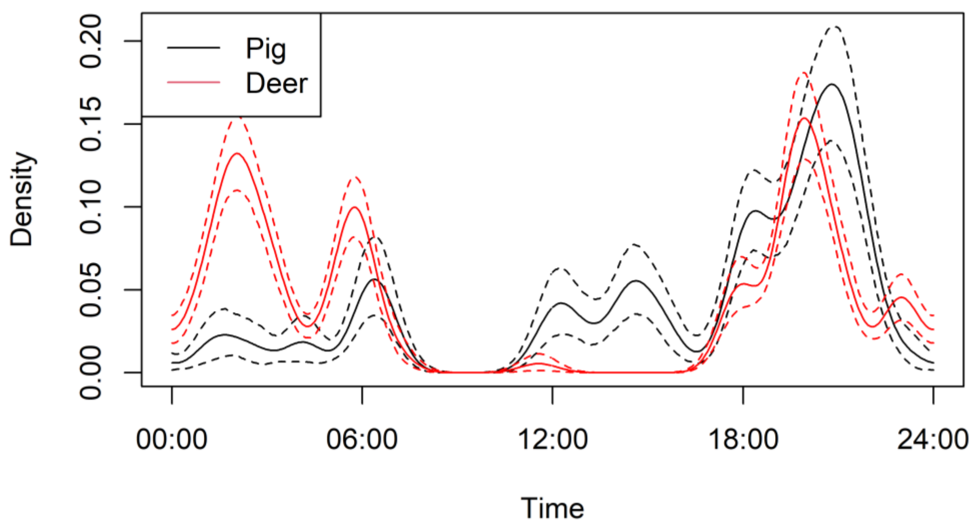


Appendix I, Figure 2. Activity level for pigs (black) and deer (red) from Tarague camera trap data. Dotted lines are 95% confidence intervals computed from bootstrap methods.

midday. For the Tarague dataset, the sampling period for both species should include detections from the five-hour peak activity period (17:00 to 22:00 h).

Anna Staudenmaier (Department of Land and Natural Resources, Rota; written communication, 27 July 2021) found that peak activity of deer on Rota was similar to that in the Naval Munitions Station Fence #1 trail camera trap data but differed from deer peak activity periods in the Tarague camera trap study. The differences in the peak activity periods among these three studies indicates that to avoid bias, sampling periods should be derived for species- and location-specific camera trap studies.

**References**

Rowcliffe, J. M. 2021. Activity: animal activity statistics. R package version 1.3.1.

## Appendix II: R Code

The following R code was used for modeling activity levels and estimating density using distance sampling for camera trap (CTDS) methods. Although these data have been processed successfully on a computer system at the U.S. Geological Survey (USGS), no warranty expressed or implied is made regarding the display or utility of the data for other purposes, nor on all computer systems, nor shall the act of distribution constitute any such warranty. The USGS or the U.S. Government shall not be held liable for improper or incorrect use of the data described or contained herein.

**Modeling Activity Level**

CTDS methods can be sensitive to temporal variation in animal activity patterns and requires censoring the sampling period to the proportion of the day when animals are available for detection (peak activity; Howe *et al.* 2017). Animal activity patterns were modeled to determine peak levels using the R package *activity* (Rowcliffe *et al.* 2014).

```
## Temporal availability----
library(activity)
#Data is in the data.frame 'dat'

#Number of hours & proportion of time cameras operated per day
camera.operation.per.day <- 24
prop.camera.time <- camera.operation.per.day/24

#Time recorded on 24:00 clock in the Video_Time field; convert to radian time using gettime()
function
dat$TimeRad <- gettime(dat$Video_Time, "%H:%M", scale="radian")

#Apply kernal smoother using fitact() function
act_result <- fitact(dat$TimeRad, sample="data", reps=100)
plot(act_result)
print(act_result@act)

#Temporal availability multiplier for dht2() function
avail <- list(creation=data.frame(rate=act_result@act[1]/prop.camera.time,
                            SE = act_result@act[2]/prop.camera.time))

#Temporal availability multiplier for bootdht() function
mult <- list(availability=make_activity_fn(dat.pa$TimeRad, sample="data",
                                  detector_daily_duration = camera.operation.per.day))

#END SCRIPT
```

**Estimating Densities Using CTDS Methods**

```
## Density estimation----
library(Distance)
library(knitr)

#Data is in the data.frame 'dat'
```

```
#Variables----
#Determine conversion units for distance, area
conversion <- convert_units("meter", NULL, "hectare")

#Length of snapshot moment, in seconds, used for calculating effort
Snapshot_Int <- 2

#Number of hours & proportion of time cameras were operating per day
camera.operation.per.day <- 24
prop.camera.time <- camera.operation.per.day/24

#Assign FOV by camera make and model; measurement of each camera’s field of view
available from the manufacturer
viewangle.Bushnell <- 45 # degrees
samfrac.Bushnell <- viewangle.Bushnell / 360
viewangle.Moultrie <- 35 # degrees
samfrac.Moultrie <- viewangle.Moultrie / 360
#Create data.frame with Sample.Label and fraction for dht2() modeling
#Add sampling fraction to data.frame accounting for different camera make and model FOVs
samfrac <- dat %>%
  mutate(fraction = if_else(Manufacturer %in% "Moultrie",
           samfrac.Moultrie, samfrac.Bushnell)) %>%
  select(Sample.Label, fraction) %>%
  group_by(Sample.Label, fraction) %>%
  summarise() %>%
  as.data.frame()

#Explore cutpoints (example cutpoints provided)
breakpoints <- c(seq(0,5,1), 8, 10)
#breakpoints <- c(0, 2, seq(3,5,1), 8, 10)
#Drop first bin, truncate at 10 m, and group data from 5-8 m and 8-10 m
#trunc.list <- list(left=1, right=10)
#breakpoints <- c(seq(1,5,1), 8, 10)
#View distance recordings with breakpoints
ggplot(data = dat, aes(x = distance)) +
  geom_histogram(breaks = breakpoints)

#Detection function modeling----
#Example distance sampling code to fit half-normal (hn) key detection function model. Similar
models should be generated for the half-normal model with cosine and Hermite polynomial
adjustment terms, for the hazard rate (hr) key and cosine and simple polynomial adjustment
term detection functions, and the uniform (un) detection function with one and two cosine
adjustment terms.
hn <- ds(dat,
        transect="point",
        key="hn",
        adjustment=NULL,
        monotonicity=FALSE,
        convert_units=conversion,
        er_var="P3",
```

```
        #truncation=trunc.list,
        cutpoints=breakpoints)
#Model checking
 gof_ds(hn)
check.mono(hn$ddf, plot=TRUE, n.pts=100)
plot(hn)
plot(hn, pdf=TRUE)
summary(hn)

#Make an AIC summary statistics table for detection function models
summarize_ds_models(hn,
                    hn.cos,
                    hn.poly,
                    hr,
                    hr.cos,
                    hr.poly,
                    un.cos1,
                    un.cos2,
                    sort="AIC", delta_only=FALSE, output="plain")

#Overdispersion----
chat <- function(modobj) {
  #  computes c-hat for a dsmodel object using Method 1 of Howe et al. (2019)
  test <- gof_ds(modobj)
  num <- test$chisquare$chi1$chisq
  denom <- test$chisquare$chi1$df
  chat <- num/denom
  return(chat)
}

qaic <- function(modobj, chat) {
  #  computes QAIC for a dsmodel object given a c-hat
  value <- 2* modobj$ddf$ds$value/chat + 2 * (length(modobj$ddf$ds$pars)+1)
  return(value)
}

qaic.pass1 <- function(...) {
  #   Performs Pass 1 model selection based upon Method 1 of Howe et al. (2019)
  #   Arguments are dsmodel objects; assumed all based on same key function
  #    c-hat is computed for the most parameter-rich model in the group
  #    qaic is calculated for each model in group based upon this c-hat
  #   Result returned in the form of a data.frame with model name, npar, aic and qaic
  models <- list(...)
  num.models <- length(models)
  npar <- unlist(lapply(models, function(x) length(x$ddf$ds$par)))
  modname <-  unlist(lapply(models, function(x) x$ddf$name.message))
  aic <-  unlist(lapply(models, function(x) x$ddf$criterion))
  chat.bigmod <- chat(models[[which.max(npar)]])
  qaic <- vector(mode="numeric", length = num.models)
  for (i in 1:num.models) {
    qaic[i] <- qaic(models[[i]], chat.bigmod)
```

```
  }
  nicetab <- data.frame(modname, npar, aic, qaic)
  return(nicetab)
}

winners <- list(hn, hr, hr.cos)   # list the detection function models to evaluate; 3 in this example
chats <- unlist(lapply(winners, function(x) chat(x)))
modnames <- unlist(lapply(winners, function(x) x$ddf$name.message))
results <- data.frame(modnames, chats)
results.sort <- results[order(results$chats),]
knitr::kable(results.sort, digits=2, row.names = FALSE)

# Density estimates----
#Need this for dht2 to work, pulled the code from
http://examples.distancesampling.org/Distance-cameratraps/camera-distill.html
dat$object[!is.na(dat$distance)] <- 1:sum(!is.na(dat$distance))
#Temporal availability multiplier, avail, computed above in Modeling activity levels.
dens <- dht2(hr,
        flatfile=dat,
        #strat_formula=~1,
        strat_formula=~Region.Label,
        stratification="geographical",
        sample_fraction=samfrac,
        er_est="P3",
        multipliers=avail,
        convert_units=conversion)
print(dens, report="density")

#Bootstrap procedures----
#In the bootstrap procedure we treat each camera trap site as the sampling unit, a product of
the systematic random sampling design, and set the resample_transects argument to true. The
camera trap sites have transect length of zero, an inherited product of point transect distance
sampling.
#Function to keep density estimates produced by each bootstrap
#Example function when there are strata and both densities and abundances are kept
NDhats <- function(ests, fit) {
  ns <- ests$individuals$N
  ds <- ests$individuals$D
  foo <- as.data.frame(matrix(ns$Estimate, nrow = 1))
  names(foo) <- make.names(paste0("N.", ns$Label), unique = TRUE)
  bar <- as.data.frame(matrix(ds$Estimate, nrow = 1))
  names(bar) <- make.names(paste0("D.", ds$Label))
  return(cbind(foo, bar))
}
#Example function when no strata are included and just densities are kept
mysummary <- function(ests, fit){
   return(data.frame(Dhat = ests$individuals$D$Estimate))
}
```

#Bootstrapping procedures took up to two hours to run given the AAFB deer and pigs datasets. Example code using the hazard rate key detection function model. Temporal availability multiplier, mult, computed above in Modeling activity levels.

```
boot <- bootdht(model=hr,
            flatfile=dat,
            resample_transects=TRUE,
            nboot=1000,
            summary_fun=NDhats,
            sample_fraction=samfrac,
            multipliers=mult,
            convert_units=conversion)

#Plot density estimates multiple strata
par(mfrow=c(1,2))
hist(boot$D.Plateau, breaks = 20,
    xlab="Estimated density", main="Plateau")
abline(v=quantile(boot$D.Plateau, probs = c(0.025,0.975),
              na.rm=TRUE), lwd=2, lty=3)
abline(v=quantile(boot$D.Plateau, probs = c(0.5),
              na.rm=TRUE), lwd=2, lty=1)
hist(boot$D.Tarague, breaks = 20,
    xlab="Estimated density", ylab=NULL, main="Tarague")
abline(v=quantile(boot$D.Tarague, probs = c(0.025,0.975),
              na.rm=TRUE), lwd=2, lty=3)
abline(v=quantile(boot$D.Tarague, probs = c(0.5),
              na.rm=TRUE), lwd=2, lty=1)
par(mfrow=c(1,1))

#Plot density estimate single stratum
hist(boot$Dhat, breaks = 20,
     xlab="Estimated density", main="D-hat estimates bootstraps")
abline(v=quantile(boot$Dhat, probs = c(0.025,0.975),
              na.rm=TRUE), lwd=2, lty=3)
abline(v=quantile(boot$Dhat, probs = c(0.5),
              na.rm=TRUE), lwd=2, lty=1)

# Compute total densities from bootstrap output----
# assign bootstrap object to dboot
dboot <- data.frame(boot)
# compute the average density weighted by stratum area
area_plateau <- 985
area_tarague <- 410
area_total <- area_plateau + area_tarague
dboot$D.wtavg <- (area_plateau * dboot$D.Plateau + area_tarague *
dboot$D.Tarague)/area_total
# assign summary statistics
dboot.median <- as.data.frame(apply(dboot, 2, median))
dboot.mean <- as.data.frame(apply(dboot, 2, mean))
dboot.se <- as.data.frame(apply(dboot, 2, sd))
dboot.bll <- as.data.frame(apply(dboot, 2, quantile,
                          probs=0.025))
```

```
dboot.bul <- as.data.frame(apply(dboot, 2, quantile,
                                 probs=0.975))
dboot.summ <- cbind(dboot.median, dboot.mean, dboot.se,
                    dboot.bll, dboot.bul)
dboot.summ <- data.frame(dboot.summ)
colnames(dboot.summ) <- c('median', 'mean', 'se', 'bll', 'bul')
dboot.summ <- dboot.summ[-c(6,7), ]

kableExtra::kbl(dboot.summ, align = 'l', digits=2) %>%
  kableExtra::kable_classic(html_font = "Cambria")

# END SCRIPT
```

**References**


Howe, E. J., S. T. Buckland, M.-L. Despres-Einspenner, and H. S. Kühl. 2017. Distance sampling with camera traps. Methods in Ecology and Evolution 8:1558–1565.

Howe, E. J., S. T. Buckland, M.-L. Despres-Einspenner, and H. S. Kühl. 2019. Model selection with overdispersed distance sampling data. Methods in Ecology and Evolution 10:38–47.

Rowcliffe, J. M., R. Kays, B. Kranstauber, C. Carbone, and P. A. Jansen. 2014. Quantifying levels of animal activity using camera trap data. Methods in Ecology and Evolution 5:1170–1179.

## **Appendix III: Example Snapshot Moments**

Example snapshot moments of deer (Appendix III, Figure 1) and pigs (Appendix III, Figure 2) where an animal was observed next to a reference flag staked out in 1-m intervals from both day and night detections. We treated these distance measurements as truth (human-based) and compared with automated-based distance estimates to evaluate automated distance estimate accuracy.


Appendix III, Figure 1. Detections of deer at known locations during diurnal (left image) and nocturnal (right image) periods. In the diurnal snapshot moment, the manually estimated distance was 2.5 m, which was placed to the 2–3 m distance interval and assigned a distance of 2 m. The automated distance estimate was 3.29 m and assigned a distance of 3 m. The deer in the nocturnal snapshot moment was manually assigned a distance of 2 m, whereas the automated-based estimate was 2.09 m and also assigned a distance of 2 m.


Appendix III, Figure 2. Detections of pigs at known locations during diurnal (left image) and nocturnal (right image) detections. The distance to the pig in the diurnal snapshot moment was manually estimated at 2.5 m, was placed to the 2–3 m distance interval, and assigned a distance of 2 m. The automated distance estimate was 3.64 m and assigned a distance of 3 m. In the nocturnal snapshot moment, the manually estimated distance was 2 m, was placed to the 2–3 m distance interval, and assigned a distance of 2 m. The automated-based distance estimate was 2.41 m and assigned a distance of 2 m.

## APPENDIX IV: BEST PRACTICES FOR CONDUCTING DISTANCE SAMPLING WITH CAMERA TRAP SURVEYS AND DENSITY ESTIMATION

### Camera Trap Layout

- Deploy cameras at regular intervals on a grid with randomized starting points to ensure the layout of cameras is random relative to the target species distribution.
- We used a 500- x 500-m regular sized trapping grid that is generalizable. This grid can be scaled to accommodate additional camera traps to minimize estimator uncertainty and expanded to survey deer and pigs in other areas of Andersen Air Force Base as well as elsewhere on Guam.

### Adequate Coverage

- Sampling at more locations than used in this study (either all grid points in Plateau stratum or sampling at a higher density) would be needed to reach the desired lower coefficients of variation (CVs).
- Palencia *et al.* (2021) noted to reduce the number of cameras needed for a high-density grid, one can use a moving approach where camera traps are first deployed to one subset of the grid (e.g., every other point) then moved to a new location (e.g., remaining points). An alternative approach is to sample more of the trap sites by rotating the orientation of each camera as done in this study.
- Increasing the number of cameras would be warranted especially if populations decline from management activities like hunting.
- Optimizing camera trap spacing for one species will over or under sample for another species. Therefore, do not optimize placement for any one species. Or, if optimizing is preferred, treat each species as a separate study. The behavior of deer and pigs on Guam likely is similar enough to not require species-specific sampling designs.

### Camera Trap Placement

- Cameras should have highly sensitive passive infrared motion sensors that can be set to medium range and take high-quality videos (1280 x 720 pixels per frame at 20 fps images).
- Video recording length should be consistent among all cameras. We used 15-second-long videos. Trigger times should be programmed to trigger immediately, and the delay between detections when an animal remains in range should be programmed to 0 seconds.
- Cameras should be secured to trees 30–50 cm above the ground and angled parallel to the slope of the ground to record animals throughout the field of view (FOV). Haucke *et al.* (2022) suggests that the bottom third of the FOV should be covered by the ground.
- Digital cameras should be operated continuously and collect video images when motion is detected by passive infrared sensors.
- Fonteyn *et al.* (2020) recommends cutting back grasses and vegetation within a 3-m radius of the camera to reduce false triggers and ensure detection is certain at zero distance. The undergrowth should, however, remain mostly unchanged. Modification within the FOV should be recorded.

- Kolowski and Forrester (2017) and Fonteyn *et al.* (2020) found sampling preferentially on game trails did not alter the detection probability or density estimates. Nonetheless, the best practice is to not sample game trails preferentially—low detection can be mitigated with longer sampling periods. Several factors other than game trails can affect detection probability (animal activity, terrain, vegetation, weather), which can be modeled during distance sampling analysis.

**Reference Distances**

- Until automated methods improve, reference distances should be collected to aid manual methods to estimate distances.
- Placing survey flags from 1 to 15 m out, at 1-m intervals, and marking natural objects (trees and branches) at known distances from the camera allowed for quick distance references for animals close to cameras and near the centerline.
- Recording a person showing a paper sheet depicting the distance to the camera (e.g., a 4 for 4 m out) and walking across the FOV from one side to the other between 1 and 11 m helped identify distances to cameras when animals were at the edges of the FOV.

**Peak Activity**

- Use all videos collected to estimate densities rather than meeting the synchrony assumption by sub-setting the digital data to peak activity periods. Take animal activity into account by computing the level of temporal activity with variance.
- If a peak activity interval is used, it should be estimated for each study rather than using the peak activity interval from previous studies or areas.

**Sampling Period**

- Deer and pig detectability likely changes between dry and wet seasons. Sampling during both seasons is beneficial. Given this, CTDS will provide an average density across the sampling period. Cameras are needed that can withstand a tropical rainy season.

**Trapping Effort**

- Detection functions should be run on a minimum of 75 to 100 detections. This minimum number of detections was met after 3 days for deer and 2 days for pigs. Sampling for two weeks is recommended to optimize collecting when daily detection rates increased the most for both deer and pigs and to ensure adequate detections.
- Exclude detections that occurred on days of camera setup and teardown, following recommendations from Howe *et al.* (2017). Based on this study, detections on the first day after setup should also be dropped.

**Microsite and Orientation**

- Sampling at additional orientations, such as sampling all four cardinal directions, likely would yield larger gains in estimator precision than just increasing the number of camera trap locations. This is due to better capturing the microsite variation when using more orientations.

**Camera Field of View**

- Differences between FOV specified by the camera manufacturer in their manual and the actual FOV measured empirically can differ by 10 degrees or more, which can bias density estimates lower (Corlatti *et al.* 2020). Additionally, natural features such as vegetation can further restrict FOV. Therefore, the best approach is to measure FOV for each camera in the field and use that value when calculating densities.

- Animals can react to the camera and run away, biasing estimates. Not using the first second of recording by defining the snapshot interval in odd numbers (i.e., 1, 3, 5… seconds, as recording starts at 0 seconds) helps account for animal movement.

**Imagery Processing**

- All images should be assigned a unique identifier or code, which may be gathered from standard camera metadata. For this study we used CameraSiteOrientation_VideoNumber.Filetype_SnapshotMoment (e.g., CT177N_MFDC0017.AVI_M1).
- Species and object identification should follow standard naming conventions, including genus and species.
- Total number of individuals in imagery should be recorded, particularly if multiple individuals are in a single image.
- Images should be coded once for each species if multiple species occur in an image.
- Software programs and management of data protocols should be described.

**Automated Processing**

- For automated object classification, use a model that has been trained on species morphologically similar to species of interest. For pigs and deer on Guam, the European model offered by Zamba worked well.
- Automated distance estimation models worked moderately well, but manual estimation was required for more than one-third of the snapshot moments in this study. Manual estimation of distance is likely needed for now, as some programming experience is required to use current automated algorithms. The automated process is likely to improve in the next few years and become more user friendly.
- Accuracy statistics should be computed to enable evaluating the model performance on the study specific dataset. Some amount of manual classification is needed to generate these accuracy statistics (to be able to assess the rate of false negatives and false positives). Standard accuracy statistics for machine learning object classification are top 1 accuracy, precision, recall, and F1. Refer to Methods, Accuracy Statistics in the main text and the following URLs:
    - Accuracy: https://developers.google.com/machine-learning/crash-course/classification/accuracy
    - Precision and Recall: https://developers.google.com/machine-learning/crash-course/classification/precision-and-recall
    - F1: https://en.wikipedia.org/wiki/F-score

**Analyses**

- Camera trap days or nights should be calculated by summing the number of 24-h periods each camera per site was operating.
- Researchers should record the number of images (1) taken, (2) per camera per site, and (3) with objects, broken down by target and non-target objects, and blanks (empty images that do not contain visible objects).

- Analyses to estimate the level of temporal activity with variance and density with variance using CTDS methods can be carried out in the R statistical program using scripts available in Appendix II.
- Input data include CSV files of a camera operation (or SD card) log and detections with distances.
- Camera operation log includes fields for camera identification, strata, start time and date, end time and date, and FOV. If data are collected from multiple orientations, the start and end information should be specific to each orientation.
- The file of detections with distances should also include fields for camera identification, video name, video time and date, snapshot moment, object, and distance.
- From the camera operation log, compute effort, independently by orientation if needed.
- Combine camera operation log with effort to the detections with distances file.
- Compute temporal activity.
- Conduct conventional distance sampling.
- Compute Akaike's information criterion (AIC) statistics.
- Compute overdispersion.
- Select best-fit model based on AIC and overdispersion values.
- Compute densities using *dht2* function.
- Perform bootstrap procedures.
- Plot and table results.

**References**

Corlatti, L., S. Sivieri, B. Sudolska, S. Giacomelli, and L. Pedrotti. 2020. A field test of unconventional camera trap distance sampling to estimate abundance of marmot populations. Wildlife Biology 2020(4):wlb.00652. https://doi.org/10.2981/wlb.00652

Fonteyn, D., C. Vermeulen, N. Deflandre, D. Cornelis, S. Lhiest, F. G. A. Houngbegnon, J.-L. Doucet, and A. Fayolle. 2020. Wildlife trail or systematic? Camera trap placement has little effect on estimates of mammal diversity in a tropical forest in Gabon. Remote Sensing in Ecology and Conservation DOI: 10.1002/rse2.191.

Haucke, T., H. S. Kühl, J. Hoyer, and V. Steinhage. 2022. Overcoming the distance estimation bottleneck in camera trap distance sampling. arXiv:2105.04244v1.

Howe, E. J., S. T. Buckland, M.-L. Despres-Einspenner, and H. S. Kühl. 2017. Distance sampling with camera traps. Methods in Ecology and Evolution 8:1558–1565.

Kolowski, J. M., and T. D. Forrester. 2017. Camera trap placement and the potential for bias due to trails and other features. PLoS ONE 12:e0186679. https://doi.org/10.1371/journal.pone.0186679

Palencia, P., J. M. Rowcliffe, J. Vicente, and P. Acevedo. 2021. Assessing the camera trap methodologies used to estimate density of unmarked populations. Journal of Applied Ecology DOI: 10.1111/1365-2664.13913.